

**Development of Flame Retardant Cotton Fabrics
with Multifunctional Properties**

Asif Javed, MSc.

SUMMARY OF THE THESIS

Title of the thesis: **Development of Flame Retardant Cotton Fabrics with Multifunctional Properties**
Author: **Asif Javed, M.Sc.**
Field of Study: **Textile Technics and Material Engineering**
Mode of Study: **Full Time**
Department: **Material Engineering**
Supervisor: **Ing. Jana Saskova, PhD.**

Committee for defense of the dissertation:

Chairman:
prof. Dr. Ing. Zdeněk Kůs FT TUL, Department of Clothing Technologies

Vice Chairman:
doc. Ing. Vladimír Bajzík, Ph.D. FT TUL, Department of Textile Evaluation
doc. Ing. Stanislav Petřík, CSc. (opponent) CXI TUL, Department of Advanced Materials
doc. RNDr. Jiří Vaníček, CSc.
doc. Ing. Martina Viková, Ph.D. FT TUL Department of Material Engineering
Ing. Michal Černý, Ph.D. University of Pardubice, Faculty of Chemical Technology, Department of Synthetic Polymers, Fibres and Textile Chemistry

Ing. Josef Večerník, CSc. Večerník s.r.o.

opponent who is not a member of the committee
doc. Mgr. Barbora Lapčíková, Ph.D. T. Bata University in Zlín, Faculty of Technology

The dissertation is available at the Dean's Office FT TUL.

Liberec 2024

ABSTRACT

Cotton's unique qualities, such as hydrophilicity, biodegradability, durability, high dye-ability, and comparatively low cost, make it a popular textile fabric. However, in contemporary times, people desire cotton fabric to possess multifunctional qualities that can provide safety based on the work place environment and weather conditions. The demand in the market has shifted towards flame retardant, UV protection, self-cleaning, antibacterial, permanently stiff textiles, and extensive studies are being conducted in these fields. Nanoparticles (NPs), for example, zinc oxide (ZnO), titanium dioxide (TiO₂), magnesium oxide (MgO), copper oxide (CuO), carbon nanotubes, silicon dioxide (SiO₂), and silver (Ag), exhibit remarkable functional properties. Among the various nanoparticles, zinc oxide (ZnO) emerges as the most environmentally friendly and relatively cost-effective option. ZnO can be applied to diverse substrates, including textile polymers and fabrics. Researchers have utilized different approaches for the deposition of ZnO NPs onto the fabric surface, such as in-situ synthesis and ex-situ deposition. However wash durability of the coated fabric is of great concern, moreover environmentally friendly, ecological functionalization of fabrics is the main demand of the present era.

The aim of the present research work is to develop a halogen and formaldehyde free ecological and durable flame retardant fabric along with multifunctional properties and to find the optimal conditions and parameters. In this research work, ZnO NPs were grown onto 100 % cotton fabric using the sonochemical method. Zinc acetate dihydrate (Zn(CH₃COO)₂·2H₂O) and sodium hydroxide (NaOH) were used as precursors. After ZnO NPs growth N-Methylol dime-thylphosphonopropionamide (MDPA) flame retardant was applied in the presence of 1, 2, 3, 4-butanetetracarboxylic acid (BTCA) as a cross linker and sodium hypophosphite (SHP) as a catalyst by conventional pad dry cure method. Induced coupled plasma atomic emission spectroscopy (ICP-AES) was used to determine the deposited amount of Zn contents % and phosphorous (P) contents %. Scanning electron microscopy (SEM), X-ray powder diffraction (XRD), and Fourier-transform infrared spectroscopy (FTIR) were employed to determine the surface morphology and characterization of developed samples. Furthermore, the thermal degradation of untreated sample and treated samples was investigated by thermo gravimetric analysis (TGA). Furthermore, the vertical flame retardant test, limiting oxygen index (LOI), ultraviolet protection factor (UPF), antibacterial activity, self-cleaning ability, and wash durability of samples were examined. The developed samples showed excellent results for self-cleaning, flame retardancy (i.e. 39 mm char length, 0 second after flame time, 0 second after glow time), 32.23 LOI, 143.76 UPF, 100 % antibacterial activity. The developed samples showed good wash durability. Additionally, the bending rigidity, air permeability and tensile strength of the developed samples were measured. The developed samples showed an increase in bending rigidity while a decrease in air permeability and tensile strength. Statistical analysis of obtained data revealed that all process parameters have a significant effect on the properties of the developed samples.

Keywords: Flame retardants, antibacterial, ZnO, nanoparticles, metal oxide

ABSTRAKT

Jedinečné vlastnosti bavlny, jako hydrofilita, biodegradabilita, trvanlivost, dobrá barvitelnost a relativně nízká cena, z ní činí oblíbenou textilií. V současné době však lidé touží po tom, aby bavlněná tkanina měla multifunkční vlastnosti, které mohou poskytnout větší komfort na základě pracovního prostředí a povětrnostních podmínek. Poptávka na trhu se posunula směrem k nehořlavosti, UV ochraně, nemačkovosti, samočisticím a antibakteriálním vlastnostem. V těchto oblastech probíhají rozsáhlé studie. Nanočástice (NP), například oxid zinečnatý (ZnO), oxid titaničitý (TiO₂), oxid hořečnatý (MgO), oxid měďnatý (CuO), uhlíkové nanotrubičky, oxid křemičitý (SiO₂) a stříbro (Ag), vykazují pozoruhodné funkční vlastnosti. Mezi různými nanočásticemi se využití oxidu zinečnatého (ZnO) jeví jako nejekologičtější a nejekonomičtější možnost. Zároveň jej lze aplikovat na různé substráty včetně textilních polymerů a tkanin. Vědecké práce popisují různé přístupy k depozici nanočástic oxidu zinečnatého na povrch taniny, jako například syntéza in-situ a depozice ex-situ. Hlavním požadavkem dnešní doby je ekologická a přírodu nezatěžující funkcionalizace tkanin a u povrchově upravených tkanin je důležitá i stálost v praní.

Cílem této výzkumné práce je vyvinout ekologicky upravenou a trvale nehořlavou tkaninu bez obsahu halogenů a formaldehydu s multifunkčními vlastnostmi a nalézt optimální podmínky a parametry. V této výzkumné práci byly nanočástice oxidu zinečnatého vyvíjeny na 100% bavlněné tkanině pomocí sonochemické metody. Jako prekurzory byly použity dihydrát octanu zinečnatého (Zn(CH₃COO)₂·2H₂O) a hydroxid sodný (NaOH). Po růstu nanočástic ZnO byl metodou pad-dry aplikován zpomalovač hoření N-methyloldimethylfosfonopropionamid (MDPA). Jako zesilující činidlo byla použita 1, 2, 3, 4-butantetrakarboxylová kyselina (BTCA) a jako katalyzátor fosforan sodný (SHP). Pro stanovení množství procentuálního obsahu zinku a fosforu byla použita atomová emisní spektroskopie s indukovaným vázaným plazmatem (ICP-AES). Pro charakterizaci vyvinutých vzorků a sledování povrchu byly použity rastrovací elektronová mikroskopie (SEM), prášková rentgenová difrakce (XRD) a infračervená spektroskopie s Fourierovou transformací (FTIR). Dále byla zkoumána tepelná degradace neupraveného vzorku a ošetřených vzorků termogravimetrickou analýzou (TGA). Byly též provedeny vertikální testy retardéru hoření, a stanoveno limitní kyslíkové číslo (LOI), byl zkoumán UPF faktor (ochrana proti ultrafialovému záření), antibakteriální aktivita, samočisticí schopnost a stálost v praní. Vyvinuté vzorky vykazovaly vynikající výsledky pro samočištění, zpomalení hoření (tj. 39 mm délka spáleného vzorku, 0 s doba dohoření, 0 s doba dosvitu), 32,23 LOI, 143,76 UPF, 100% antibakteriální aktivita. Vyvinuté vzorky vykazovaly i dobrou stálost v praní. Dále byla měřena tuhost v ohybu, propustnost vzduchu a pevnost v tahu vyvinutých vzorků. Bylo prokázáno zvýšení ohybové tuhosti při současném snížení propustnosti vzduchu a pevnosti v tahu. Statistická analýza získaných dat ukázala, že všechny parametry procesu mají významný vliv na vlastnosti vyvinutých vzorků.

Klíčová slova: Zpomalovače hoření, antibakteriální, ZnO, nanočástice, oxidy kovů

TABLE OF CONTENTS

ABSTRACT	III
ABSTRAKT	IV
1. Introduction	1
2. Purpose and aims of the thesis	2
3. Overview of the current state of the problem	3
4. Methods used, studied materials	4
4.1. Materials	4
4.2. Surface activation of cellulose.....	4
4.3. In-situ sonochemical synthesis of ZnO NPs on cotton fabric.....	5
4.4. Extraction of solid powder	6
4.5. MDPA application	6
4.6. Characterization and testing.....	8
4.6.1. Content analysis	8
4.6.2. Add-on %	8
4.6.3. Surface morphology	8
4.6.4. Particle size analysis	8
4.6.5. XRD analysis	8
4.6.6. FTIR analysis	8
4.6.7. Thermogravimetric analysis.....	9
4.6.8. Vertical flame test	9
4.6.9. Limiting oxygen index	9
4.6.10. UV protection	9
4.6.11. Antibacterial activity.....	10
4.6.12. Self-cleaning	10
4.6.13. Bending rigidity	10
4.6.14. Air permeability.....	10
4.6.15. Tensile strength.....	11
4.6.16. Wash durability.....	11
5. Summary of the results achieved	11

5.1.	Content analysis	11
5.2.	SEM analysis	13
5.3.	Particle size	14
5.4.	XRD analysis	15
5.5.	FTIR analysis	16
5.6.	Thermo gravimetric analysis	17
5.7.	Vertical flame test	19
5.8.	Limiting oxygen index (LOI)	22
5.9.	Antibacterial activity	24
5.10.	Ultraviolet protection factor (UPF)	27
5.11.	Self-cleaning.....	29
5.12.	Bending rigidity	32
5.13.	Air permeability	36
5.14.	Tensile strength	38
5.15.	Wash durability	40
6.	Evaluation of results and new findings	43
7.	References	44
8.	List of Publications.....	53
	Curriculum Vitae.....	55
	Recommendation of Supervisor	56
	Reviews of the Opponents.....	57

1. Introduction

Fire has claimed more deaths in the United States than all other natural incidents combined. The National Fire Protection Association (NFPA) disclosed that there were 1.35 million fires in the United States in 2009, which resulted in 3010 fatalities, 17,050 human injuries, and a \$12.53 billion loss of assets. Surprisingly, residential structures accounted for 28% of all fires and caused the majority of the damage[1]. According to reports, furniture with upholstery, mattresses, and bedding fires caused 70% of the fatalities associated with household smoking material flames[2]. Thus, the flame retardant coating of textile-based items can greatly help to save lives as well as property in residential buildings[3], [4].

Cotton fiber is among the most plentifully used fibers all over the world. It is comfortable, cozy, and breathable when used in garment form [5], [6]. However, it is one of the most combustible and very susceptible to thermal decomposition. It exhibits a very lower limiting oxygen index (approximately 17-18), as well as it is a highly flammable fiber. It burns very quickly with a hot flame and little spark [7], [8]. Moreover, with flammability and combustibility, cotton fabric provides an indigent defence to human skin against UV radiation and bacterial growth. Wearable cotton textile goods effectively absorb perspiration, sebum, and other skin secretions, a property that makes it easier for bacterial growth. This bacterial breeding is directly linked to a number of newly developing infections or diseases that are currently gaining attention in the global public health arena. Therefore these are the fundamental problems for the cotton fabric, limiting its use in industrial work wear, housing, and technical applications [9], [10].

Flame retardant treatment on textile fabrics has gained significant importance because flame retardant fabrics can be used as safety work wear in industry, firefighting wears, in hospitals, and as in household upholstery [11], [12]. Various chemical applications are involved in producing flame retardant fabrics, but most of the flame retardant chemicals contain halogen compounds that are not environmentally friendly [13], [14]. Halogen-based compounds produce hazardous fumes and gases that affect the endocrine system. The findings of some studies caused the manufacturing of two main classes, notably polybrominated diphenyl ethers (PBDEs) and polybrominated biphenyls (PBB), to be banned in the EU and the USA. All of this occurred as a result of increasing findings that PBDEs accumulate in biological organisms and remain in the environment. Additionally, toxicological tests revealed that these compounds may be hazardous to the neural systems and cause deleterious effects on the thyroid, and liver. PBBs have been reported to be carcinogenic to the liver of mice and rats. As per the findings of the Department of Health and Human Services (DHHS) PBBs could be harmful to human health in terms of cancer. Phosphorous based durable flame retardant chemicals are alternatives to halogen compounds. These phosphorous based compounds are ecological, environmentally friendly and economical for cotton textile applications [15]. In a study Cheema *et al.* treated cotton fabric with N,N-dimethyl di(acryloyloxyethyl) phosphoramidate (DMAEP), a halogen free phosphorous and nitrogen based chemical for flame retardancy. They achieved excellent flame retardancy along with increased char formation[7]. In one more study Gall *et al.* fabricated cotton, cotton/polyester, and cotton/polyamide surfaces by coating water soluble cyclophosphazene as a flame retardant finish and reported the increase in flame retardancy, increase in limiting oxygen index, as well as the formation of the glassy insulating layer on the substrate [8]. In an other study Zhang *et al.* achieved improved flame

retardancy of cellulose fibers by grafting zinc ion along with N,N-dimethylformamide (DMF) application[11]. Li *et al.* synthesized a halogen free flame retardant for cotton fabric containing –P–O–NH₄⁺ groups and achieved excellent results for flame retardancy[16]. Chen *et al.* synthesized poly lactic acid (PLA) and phosphazene/triazine bi-group composite along with doping of zinc oxide nanoparticles (ZnO NPs) and achieved excellent flame retardancy, higher limiting oxygen index, and increased char residues[17].

N-methylol dimethyl phosphonopropion amide (MDPA) is one of the most promising and ecological flame retardant compounds due to its durability, low toxicity, environmentally friendly nature and convenient application. When it is applied along with a cross linker onto the cotton fabric, it makes the covalent bond with a hydroxyl group of cotton cellulose, hence enhancing its durability[18], [19].

Nanotechnology is another most important field that has been utilized successfully and efficiently in the industry to achieve desired fruitful results. Nanomaterials in the textile industry have earned great importance due to their multipurpose uses [20]. Nanomaterials in the form of nanoparticles are being used in the textile industry for antibacterial textile [21], UV protection, to increase flame retardancy, self-cleaning, electromagnetic shielding (EMI), conductive textiles, etc. [22]–[24]. Among the nanoparticles used in industry, metal oxides are of the great importance because of their multipurpose properties [25]. Zinc oxide (ZnO) and titanium dioxide (TiO₂) are the most commonly used inorganic metal oxides in the textile industry. TiO₂ has just been categorized as an IARC group 2B carcinogen, probably harmful to humans, by the International Agency for Research on Cancer (IARC). The IARC findings are based on data demonstrating that exposure to large concentrations of pigment-grade and ultrafine TiO₂ dust results in cancer of the respiratory tract in rats. The discoveries were deemed relevant to humans by the IARC because several biological processes that result in lung cancer in rats appear to be similar to those that occur in people who work in dusty environments[26]. However, ZnO is "generally identified as safe" by the US Food and Drug Administration (FDA). ZnO is n-type semiconductor white in color, having a high refractive index with a wide band gap of 3.37 eV [27]. Along with UV protection, antibacterial, and self-cleaning properties, zinc oxide nanoparticles (ZnO NPs) are being used in flame retardant coating [28], [29]. ZnO NPs are used as co-catalyst in flame retardant finishing and are very effective in char formation during the burning of fabric [14]. Researchers showed that ZnO NPs as co-catalyst increase the flame retardancy of cotton fabric by forming a protective layer on the fabric and restricting the supply of oxygen to the fabric which is necessary for burning, as well as it also increases the durability of flame retardant [31], [32].

2. Purpose and aims of the thesis

The production of flame retardant fabrics on a wide scale using affordable, simple, and environmentally friendly methods still faces several difficulties. Research on environmentally friendly preparation techniques should be prioritized, along with studies on textile durability and mechanical stability. The general goal of this research project is to utilize halogen and formaldehyde free ecological phosphorous based chemical N-methylol dimethyl phosphonopropion amide (MDPA) and deposition of ZnO NPs on cotton textiles to create flame retardant textiles with additional capabilities (such as UV protection, self-cleaning, antibacterial, etc.).

The specific objectives are as follows;

- Deposition of ZnO NPs by ultrasonic irradiation method to achieve increased flame retardancy and multifunctional properties.
- Application of N-methylol dimethyl phosphonopropion amide (MDPA) to modify the surface of fabric.
- Different parameters, such as precursor concentrations and sonication time, significantly affect the deposition of ZnO NPs on the fabric. Furthermore, concentration of N-methylol dimethyl phosphonopropion amide (MDPA) affects the flame retardancy. The purpose is to optimize process parameters and to evaluate the effect of process parameters and conditions upon flame retardancy as well as other functional properties.
- Content analysis of coated fabrics by induced coupled plasma atomic emission spectrometer (ICP AES).
- Evaluation of surface morphology of nanoparticles coated fabrics by scanning electron microscopy (SEM).
- Characterization of coated fabrics by X-ray diffraction (XRD) and the fourier transform infrared spectroscopy (FTIR)
- Evaluation of thermal stability of coated fabrics by thermo gravimetric analysis.
- Evaluation of flame retardant properties from vertical flame test and limiting oxygen test (LOI).
- Evaluation of antibacterial efficacy of coated cotton fabrics against gram positive and gram negative bacteria.
- Evaluation of UV protection of coated cotton fabrics.
- Evaluation of photo catalytic self-cleaning ability by degradation of coffee stain under UV light.
- To do the statistical analysis of obtained results.
- Evaluation of coated cotton fabric against washing.

3. Overview of the current state of the problem

Currently, the primary and most significant issue and obstacle in the textile and chemical finishing sector revolves around the escalating impact of environmental and ecological elements, particularly the growing apprehensions concerning the application of flame retardants. The advancement of flame retardancy is notably impeded by the eco-toxicological and environmental factors associated with the flame retardants utilized, as well as the hazardous characteristics of substances emitted during the combustion of textiles. The main challenges in the flame retardant/ZnO NPs system are the use of halogen free flame retardant chemical, formaldehyde free cross linker, homogeneous, even, and stable deposition of ZnO NPs. Nowadays, a significant proportion of flame retardants on the market are organic compounds derived from organo-halogenated compounds. The use of phosphorus-based flame retardants presents a promising and viable alternative to halogen-based compounds for various fibers and fabrics. N-methylol dimethyl phosphonopropion amide (MDPA) stands out as a highly auspicious, halogen free, and environmentally sustainable flame retardant compound, primarily attributed to its durability, minimal toxicity, eco-friendly characteristics, and ease of use. BTCA is a formaldehyde free cross linker that can be used for cotton flame retardant systems[33]. Javed *et al.* reported that sonochemical is an advanced and economical method for the in-situ synthesis of ZnO NPs onto the

cotton fabric[34]. This technique controls the nanoparticle size, as well as ultrasonic waves disperse and deposit the nanoparticles onto the fabric more stably, homogeneously and evenly[35].

Among all properties, the integration of UV protection on flame retardant surfaces is of great concern in the present work. This is because the risks of UV radiation to induce acute and chronic illnesses when they interact with skin increased significantly in recent years. UV radiations in sunlight are a natural threat to human skin and can result in major medical issues. Additionally, certain artificial medical lights produce UV radiation. Human body exposed to UV radiation without protection can suffer from major health issues such as melanoma (skin cancer), rash, erythema (skin redness), and skin ageing. Moreover, industrial workwears along with flame retardancy, also require UV protection and protection against various bacteria. Workers related to welding are exposed to hazardous radiation along with flame sparks. During arc welding, strong ultraviolet radiations (UVR) are released into the air. These radiations contain ultraviolet radiations A (UVA), ultraviolet radiations B (UVB), and ultraviolet radiations C (UVC). Human skin is harmed worsely by the exposure to ultraviolet radiations A (UVA), ultraviolet radiations B (UVB), and ultraviolet radiations C (UVC) from a short distance in the absence of a barrier. So there is a need to develop protective work wear with multifunctional properties[35], [36].

In this research study, ZnO NPs were in-situ synthesized onto the cotton fabric by ultrasonic irradiation method. After that, MDPA flame retardant in the presence of formaldehyde free ecological cross linker BTCA was applied onto the cotton fabric by pad dry cure method. The main goal of the present work is to find the optimized parameters for in-situ sonochemical synthesis of ZnO NPs, and investigate the role of ZnO NPs in flame retardant finishing and their influence on functional properties.

To the best of the author's knowledge, this is the first study on the flame retardant application in combination with MDPA along with formaldehyde free cross linker, and ZnO NPs by sonochemical method. The finding of this study could be beneficial for application in safety textiles (welding work wear, electrical work wear, industrial work wear etc.).

4. Methods used, studied materials

4.1. Materials

The 100 percent cotton fabric with a plain weave texture, 155 g/m² density, 52 ends/inch, 28 picks/inch, and 20 tex warp count, 20 tex filling count, was acquired from the Technical University of Liberec, Czech Republic. Citric acid C₆H₈O₇, zinc acetate dihydrate (Zn(CH₃COO)₂·2H₂O), sodium hydroxide (NaOH), sodium hypophosphite (SHP), and 1, 2, 3, 4-butanetetracarboxylic acid (BTCA) chemical reagents were procured from Merk, Prague, Czech Republic. N-Methylol dimethylphosphonopropionamide (MDPA) was obtained from the Huntsman Corporation. Acramin SW acrylic-based binder was obtained from Tanatex Chemicals, The Netherlands. All the obtained chemical reagents were of analytical grade and utilized as purchased without further purification.

4.2. Surface activation of cellulose

To obtain maximum adherence of ZnO NPs and MDPA on the cellulosic structure of the cotton fabric, the cotton fabric was pretreated with a 0.5% aqueous solution of citric acid in the presence of 0.5%

sodium hypophosphite as a catalyst for cellulosic surface activation. As the citric acid and cotton fibers were added to deionized water, both were ionized, as shown in equations (1) and (2). In a further reaction, carboxylic groups of citric acid were easily attached to the hydroxyl groups on the cotton fabric, as shown in equation (3).



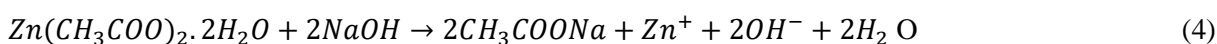
4.3. In-situ sonochemical synthesis of ZnO NPs on cotton fabric

ZnO NPs were synthesized and stabilized onto the cotton fabric concomitantly by hydrolysis of zinc acetate dihydrate ($Zn(CH_3COO)_2 \cdot 2H_2O$) and sodium hydroxide (NaOH) in deionized water. Table 1 shows the experimental variables used in this research. Full factorial experimental design was applied to develop the samples. The precursors, zinc acetate dihydrate ($Zn(CH_3COO)_2 \cdot 2H_2O$) and sodium hydroxide (NaOH) with different molar concentrations, were dissolved separately in deionized water under vigorous magnetic stirring (300 rpm) conditions. After that, the cotton fabric piece was dipped into the zinc acetate dihydrate solution for 10 min under vigorous magnetic stirring (300 rpm). After 10 min, the NaOH solution was poured dropwise into that solution at ambient temperature and under vigorous magnetic stirring (300 rpm). For absolute completion of the reaction mechanism, the obtained solution containing the immersed cotton fabric piece was sonicated for different sonication times (Table 1). The Branson sonication probe (20 kHz, 50% efficiency, 150 W) was utilized in this experimental procedure. The reaction temperature was maintained at 80 °C by utilizing a hot plate. Then, the treated fabric pieces were washed thoroughly with deionized water to remove any impurities. Eventually, the obtained fabric pieces were placed in an air oven at 90 °C for 120 min. In order to compare the sonochemical process and to accentuate the critical influence of ultrasound irradiation waves, one sample was developed using a conventional magnetic stirring method using the same precursor concentrations (0.1 M $Zn(CH_3COO)_2 \cdot 2H_2O$, 0.3 M NaOH) and temperatures (80 °C) as the optimized sample (will be discussed in next section), under vigorous magnetic stirring (300 rpm) for 90 min. In this research work, this sample was named sample A.

Equations (4–6) show the proposed mechanism of ZnO NPs synthesis on the cotton fabric.

Table 1. Experimental variables for the synthesis of ZnO NPs.

Zinc acetate dihydrate (M)	Sodium hydroxide (M)	Sonication time (minute)
0.05	0.1	30
0.1	0.2	60
0.15	0.3	90
		120



4.4. Extraction of solid powder

After removing the fabric, the solution was centrifuged at 5000 rpm for 3 min to separate the solid ZnO NPs from the liquid. The centrifuged solid was thoroughly washed with deionized water to remove any impurities and finally dried in an air oven at 90°C for 120 min.

4.5. MDPA application

MDPA application was performed with the help of a laboratory padder (Werner Mathis AG Switzerland) at 80% wet pick up. The bath formulation used 300 g/L MDPA, 60 g/L BTCA crosslinker, 50 g/L SHP catalyst, and 5 g/L acramin SW binder. Various preliminary trials were conducted to determine the best compatible concentrations of MDPA and BTCA with optimized ZnO NPs loaded samples. ZnO NPs loaded samples were impregnated in MDPA and BTCA solution, padded and dried at 110 °C for 3 min, and cured at 150 °C for 2 min. In order to determine the crucial role of ZnO NPs in flame retardancy, a cotton fabric sample was treated with MDPA and BTCA without ZnO NPs treatment. In this research work, that sample was named sample B.

Figure 1 shows the schematic diagram for surface activation of cellulose; in-situ synthesis of ZnO NPs on the cotton fabric and MDPA application and the Figure 2 indicates reaction mechanism of MDPA and BTCA with cellulose.

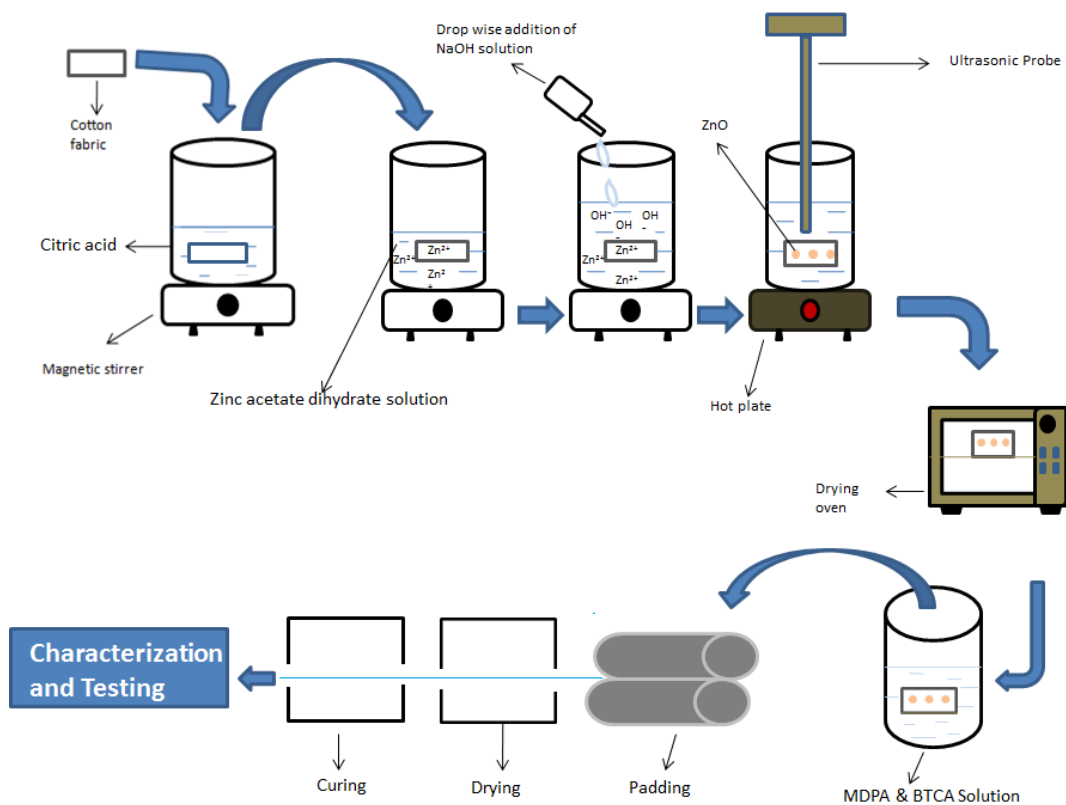


Figure 1. Schematic diagram for surface activation of cellulose, in-situ synthesis of ZnO NPs on the cotton fabric and MDPA application.

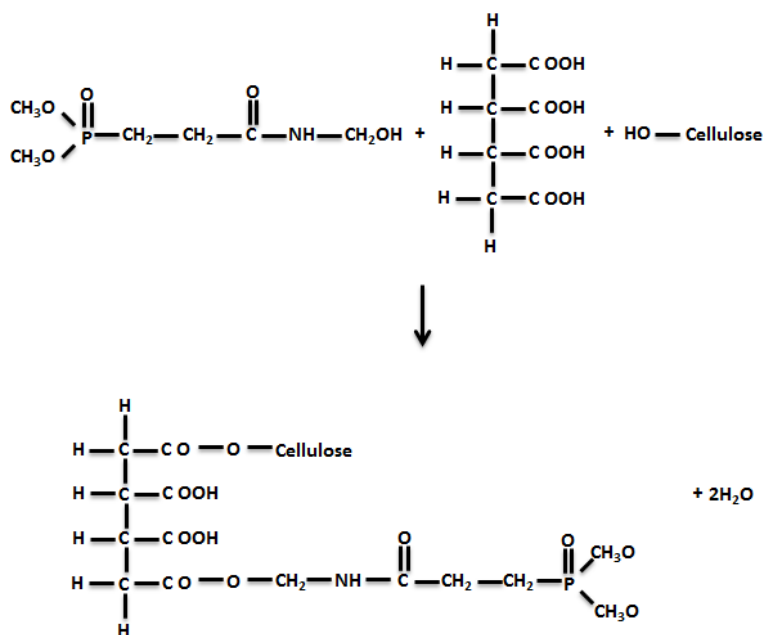


Figure 2. Reaction mechanism of MDPA and BTCA with cellulose.

4.6. Characterization and testing

4.6.1. Content analysis

The induced coupled plasma atomic emission spectrometer (ICP AES, Optima7300 DV, Perkin-Elmer Corporation, Waltham, MA, USA) was utilized to analyze the Zinc (Zn) contents and phosphorous (P) contents. The developed fabric sample of weight 0.1 g was treated with 8 mL of concentrated nitric acid (HNO₃) (65 %) until the fabric was wholly dissolved. Then the obtained solution was shifted to a volumetric flask of 100 mL capacity, and finally, dilution was done with deionized water.

4.6.2. Add-on %

The add-on % (uptake) was calculated according to equation (7).

$$Add\ on\% = \frac{w_f - w_i}{w_i} \times 100 \quad (7)$$

In equation (7)

w_f= final weight of the developed sample

w_i= initial weight of the untreated sample

4.6.3. Surface morphology

The surface of the pristine cotton and developed samples was visualized using a Quanta 200 FEG scanning electron microscope (SEM) (FEI Company, Hillsboro, OR, USA). The specimens underwent a process of gold sputter coating in order to enhance the electrical conductivity of their surface.

4.6.4. Particle size analysis

The particle size of the synthesized ZnO NPs was examined by employing dynamic light scattering (DLS) technology using the Malvern zeta sizer (Malvern Panalytical Ltd, United Kingdom). Extracted solid ZnO NPs from the synthesis solution were dispersed in deionized water with the help of an ultrasonic probe. Eventually, the DLS technique was employed.

4.6.5. XRD analysis

The XRD patterns were measured using an X-ray diffraction system (Powder X-ray diffraction system, ARL, X,TRA, Thermo Scientific USA). The measurements were recorded in the range of diffraction angle 2 Θ =10°-70°, with step size 0.02, and scan rate 2 [°/m], and 0.6 integration duration.

4.6.6. FTIR analysis

The fourier transform infrared spectroscopy (FTIR) was employed on the developed samples and pristine cotton to investigate the surface chemical structure. The measurements were performed at room temperature with the help of a Perkin Elmer spectrometer equipped with Thermo Scientific Nicolet IS50

FT-IR USA attenuated total reflectance (ATR) technology. The spectra were recorded in the range of 4000 to 400 cm^{-1} using ZnSe crystal at a resolution of 4 cm^{-1} with 32 scans.

4.6.7. Thermogravimetric analysis

The thermal stability of the developed and untreated samples was examined with the help of thermogravimetric analysis (TGA) using a TGA/SDTA 851 METLER TOLEDO analyzer. The untreated and developed samples were subjected to heat in a synthetic air atmosphere from 30 °C to 700 °C with a 10 °C/min heating rate. Finally, the weight loss percent of the samples was measured.

4.6.8. Vertical flame test

To evaluate the flammability of untreated cotton samples and developed samples, vertical flame test (ASTM D6413-2015) was employed. This particular methodology aims to ascertain the reaction of textile materials when exposed to a prescribed source of ignition. It intends to derive quantitative data regarding the duration of after flame, after glow, and the length of the resulting char.

4.6.9. Limiting oxygen index

The LOI values were recorded for untreated and developed samples according to the standard test method ASTM D2863-97. In this method, sample is ignited with combustible flame in an oxygen/nitrogen environment. The LOI measurement is conducted on specimens with dimensions (80 × 10 mm), which are positioned vertically within a glass chimney at its center. In order to achieve homogenization, the gas mixture is passed through layers of glass beads as it moves upstream through the chimney. Following a 30 seconds column purge, the specimen's upper part is ignited, resembling the lighting of a candle. Then the oxygen concentration in the oxygen/nitrogen environment is decreased until the flame is extinguished. The minimum concentration of oxygen which supports the combustion is recorded. LOI is expressed as volume percent and calculated according to the following equation (8).

$$LOI = (100 \times O_2)/(O_2 + N_2) \quad (8)$$

4.6.10. UV protection

Pristine cotton sample and treated samples were analyzed for their UV protective properties on a Varian CARY 1E UV/VIS spectrophotometer equipped with a DRA-CA-301 integration sphere and solar screen software. The samples were measured in the UV range 280 nm to 400 nm. The transmittance measurements and calculations of the UPF were carried out in accordance with the AATCC 183-2000 standard. The UPF value was calculated according to equation (9).

$$UPF = \frac{\sum_{280nm}^{400nm} E_{\lambda} S_{\lambda} \Delta_{\lambda}}{\sum_{280nm}^{400nm} E_{\lambda} S_{\lambda} T_{\lambda} \Delta_{\lambda}} \quad (9)$$

E_{λ} = solar spectral irradiance

S_{λ} = relative erythemal spectral response

Δ_{λ} = measured wavelength interval in nanometers

T_{λ} = average spectral transmittance from the sample

4.6.11. Antibacterial activity

The quantitative method AATCC 100-2012 was used to analyze the antibacterial performances of the samples. According to this standard, 1 mL of bacterial inocula was taken in a conical flask, and fabric pieces (4.8 ± 0.1 cm diameter) were added into that flask and let to remain in contact with bacterial inocula for 24 hours. After that, the solution was subjected to serial dilution up to 10^{-7} in nutrient broth. Then, the 0.1 mL of the dilution was transferred to the agar plate and finally incubated for the duration of 24 hours at a temperature of 37 °C. The no. of bacterial colonies that appeared were counted. The bacterial reduction % was calculated according to the following equation (10).

$$R\% = \frac{A-B}{A} \times 100 \quad (10)$$

Where

R= bacterial reduction %

A= no. of bacterial colonies appeared from the untreated sample

B= no. of bacterial colonies appeared from the treated sample

4.6.12. Self-cleaning

The photocatalytic self-cleaning activity of the untreated and chemically modified samples was determined based on the photodegradation of a coffee stain under UV light. For this purpose, the samples were immersed in coffee (10 g ground coffee/100 mL water) for 30 s; the stained samples were irradiated under the UV light of Philips TL 6W UV tubes (315-400 nm) and the stain degradation performance was evaluated as a function of exposure to UV light. Later, the fabric surfaces discolored after the tests were scanned with 300 dpi and the scanned images were analyzed to calculate the color intensity by Image J software.

4.6.13. Bending rigidity

Bending rigidity was measured using the TH-7 instrument. This equipment produces a bending force from which we can compute bending rigidity. The measuring range of this device for bending force is 40 mN to 4000 mN. This device is identical to the standard Kawabata KES-FB 2 device, which is used for assessing low stress mechanical properties. The mean of five readings for each sample was calculated.

4.6.14. Air permeability

The Textest FX 3300 equipment was used to assess the air permeability of untreated and developed samples in accordance with ČSN EN ISO 9237 standard. The measuring principle relies on the

measurement of the airflow passing through the fabric at a specific pressure. The airflow passing through at 200 Pa pressure on an area of 20 cm² at a range of 6 was measured. Five measurements were taken at various sites for each sample, and their averages were computed.

4.6.15. Tensile strength

Tensile strength of the samples was measured according to the test method ASTM D5034. The procedure outlined in the ASTM D5034 test method pertains to the determination of the maximum force at break for textile fabrics utilizing a grab method. The grab test, which is a form of tensile strength assessment, involves clamping the center of the specimen using mechanical clamps. Subsequently, force is applied, and the force at which the sample breaks is recorded. The Zweigle F-425 tensile tester was utilized in this research work.

4.6.16. Wash durability

The home laundering washing durability of the treated samples was examined as per ISO 105-CO6 standard. Each wash cycle of this method is equal to five home laundering. The treated samples were washed at 50 °C for 45 minutes with 4 g/L washing detergent. Finally, the washed samples were rinsed and then dried at 80 °C. Eventually, the washed samples were investigated for their functional properties.

5. Summary of the results achieved

All the results present in this research study are the mean of five replications.

5.1. Content analysis

The ICP-AES technique was employed to analyze the Zn and P contents of the developed samples and tabulated in Table 2. Zn contents analysis was done to decide the most productive and optimized sonication time and concentrations of chemical reagents. It can be seen from Table 2 that with an increased sonication time of up to 90 minutes the synthesized mass of Zn contents also increased. However, after 90 minutes the synthesized mass of Zn contents decreased. After a critical time of 90 minutes, ultrasonic waves might be led to remove the ZnO NPs from the fabric. While the higher molar concentration of NaOH leads to the higher synthesized amount of Zn contents. In the case of zinc acetate with increased concentration up to 0.1 M zinc acetate synthesized mass of Zn contents also increased. However, at 0.15 M zinc acetate synthesized mass of Zn contents tends to decrease. The maximum synthesized mass of Zn contents was achieved for sample 23, which exhibited Zn contents of 13.14 %. So, the optimal sonication time for this experiment is 90 minutes, and the optimal concentrations of the reagents are 0.1 M zinc acetate, and 0.3 M NaOH. Table 2 shows that optimized sample 23 has 3.44 phosphorous (P) contents % and 30.47 add on %. Furthermore, it can be seen from Table 2 that add on % shows the same trend as Zn contents %.

Equation (11) shows the regression model for the prediction of Zn contents %. R-squared value can be used to evaluate how well the model fits the data; the R-squared value presented in the model summary shows that the fitted model could explain 73.58 % of total variations, while the p-value = 0.00 and F-value = 80.30 presented in the model summary indicate that the model is significant.

Table 2. Experimental results for Zn contents, P contents, and add-on %.

Sample	Zinc acetate (M)	NaOH (M)	Sonication time (minutes)	MDPA (g/L)	Zn contents		P contents		Add on	
					(%)	Std. dev.	(%)	Std. dev.	(%)	Std. dev.
1	0.05	0.1	30	300	1.69	0.07	3.88	0.08	16.92	0.15
2	0.05	0.1	60	300	1.84	0.04	3.86	0.07	17.11	0.12
3	0.05	0.1	90	300	2.13	0.09	3.83	0.06	17.45	0.15
4	0.05	0.1	120	300	1.91	0.08	3.84	0.07	17.22	0.16
5	0.05	0.2	30	300	2.83	0.11	3.81	0.08	18.31	0.18
6	0.05	0.2	60	300	3.19	0.09	3.79	0.05	18.61	0.14
7	0.05	0.2	90	300	3.34	0.13	3.78	0.09	18.91	0.22
8	0.05	0.2	120	300	3.27	0.07	3.79	0.06	18.78	0.14
9	0.05	0.3	30	300	4.64	0.10	3.75	0.05	20.38	0.17
10	0.05	0.3	60	300	4.86	0.06	3.73	0.08	20.70	0.13
11	0.05	0.3	90	300	5.09	0.10	3.72	0.06	20.96	0.15
12	0.05	0.3	120	300	5.01	0.05	3.72	0.06	20.84	0.13
13	0.1	0.1	30	300	5.34	0.07	3.71	0.05	21.23	0.12
14	0.1	0.1	60	300	5.47	0.08	3.70	0.07	21.43	0.16
15	0.1	0.1	90	300	5.65	0.05	3.70	0.06	21.60	0.12
16	0.1	0.1	120	300	5.53	0.05	3.70	0.06	21.51	0.11
17	0.1	0.2	30	300	8.78	0.07	3.63	0.07	25.32	0.16
18	0.1	0.2	60	300	9.07	0.06	3.61	0.05	25.65	0.14
19	0.1	0.2	90	300	9.31	0.04	3.58	0.05	25.48	0.19
20	0.1	0.2	120	300	9.17	0.07	3.60	0.07	25.77	0.20
21	0.1	0.3	30	300	11.23	0.06	3.50	0.04	28.24	0.16
22	0.1	0.3	60	300	12.09	0.07	3.47	0.03	29.21	0.18
23	0.1	0.3	90	300	13.14	0.06	3.44	0.06	30.47	0.12
24	0.1	0.3	120	300	12.54	0.05	3.46	0.05	29.79	0.11
25	0.15	0.1	30	300	5.39	0.06	3.72	0.06	21.31	0.13
26	0.15	0.1	60	300	5.61	0.07	3.69	0.04	21.54	0.10
27	0.15	0.1	90	300	5.73	0.04	3.69	0.05	21.72	0.11
28	0.15	0.1	120	300	5.57	0.05	3.70	0.07	21.52	0.13
29	0.15	0.2	30	300	8.89	0.05	3.62	0.05	25.42	0.11
30	0.15	0.2	60	300	9.21	0.02	3.59	0.03	25.82	0.08
31	0.15	0.2	90	300	9.43	0.04	3.55	0.04	26.11	0.10
32	0.15	0.2	120	300	9.29	0.03	3.58	0.06	25.91	0.11
33	0.15	0.3	30	300	9.63	0.06	3.54	0.02	26.31	0.09
34	0.15	0.3	60	300	9.91	0.03	3.53	0.03	26.65	0.09
35	0.15	0.3	90	300	10.13	0.05	3.52	0.05	26.91	0.12
36	0.15	0.3	120	300	9.97	0.08	3.53	0.04	26.57	0.14
A	0.1	0.3	90 (magnetic stirring)	300	7.83	0.10	3.67	0.06	24.09	0.18
B	-	-	-	300	-	-	3.92	0.0	14.93	0.93

$$\begin{aligned} \text{Zn contents \%} = & -1.45 + 36.2 \text{ zinc acetate (M)} + 14.69 \text{ NaOH (M)} + 0.00001 \text{sonication time} \\ & \text{(minutes)} + 66.4 \text{ zinc acetate (M)} \times \text{NaOH (M)} - 0.0049 \text{ zinc acetate (M)} \times \text{sonication time} \\ & \text{(minutes)} + 0.0289 \text{ NaOH (M)} \times \text{sonication time (minutes)} \end{aligned} \quad (11)$$

Model summary of Zn contents %

S = 1.7058 R-squared = 73.58% R-squared (adj) = 72.66% R-squared (pred) = 71.69%
 F-Value = 80.30 p-value = 0.0000

5.2. SEM analysis

SEM Images were measured to investigate the surface morphology of the pristine cotton fabric and ZnO NPs coated samples. It can be seen from Figure 3 (a) and Figure 3 (b) that pristine cotton has a clean and smooth surface. Figures 3 (c) and 3 (d) show the SEM images for optimized sample 23, which reveals that after optimized sonochemical treatment ZnO NPs are spread onto the cotton fabric surface homogeneously, finely, and evenly. Figures 3 (c) and 3 (d) show that the surface of the fabric is entirely covered by the ZnO NPs. The deposition of ZnO NPs onto the cotton fabric surface results from attractive forces between cellulosic functional groups and ZnO NPs [38]. SEM images show that the deposition of ZnO NPs created roughness on the surface of fibers. Figure 3 (f) SEM image for sample A indicates that there is a deposition of ZnO NPs onto the cotton fabric surface after the conventional magnetic stirring method, but as compared to the sonochemical method, the ZnO NPs are not spread smoothly, finely and homogeneously. Figure 3 (e) shows the SEM image for optimized sample 23 at high resolution, showing that ZnO particles are deposited onto the cotton surface at a nano scale with narrow size distribution. Moreover, Figure 3 (e) reveals that most of the ZnO NPs have round and spherical shapes.

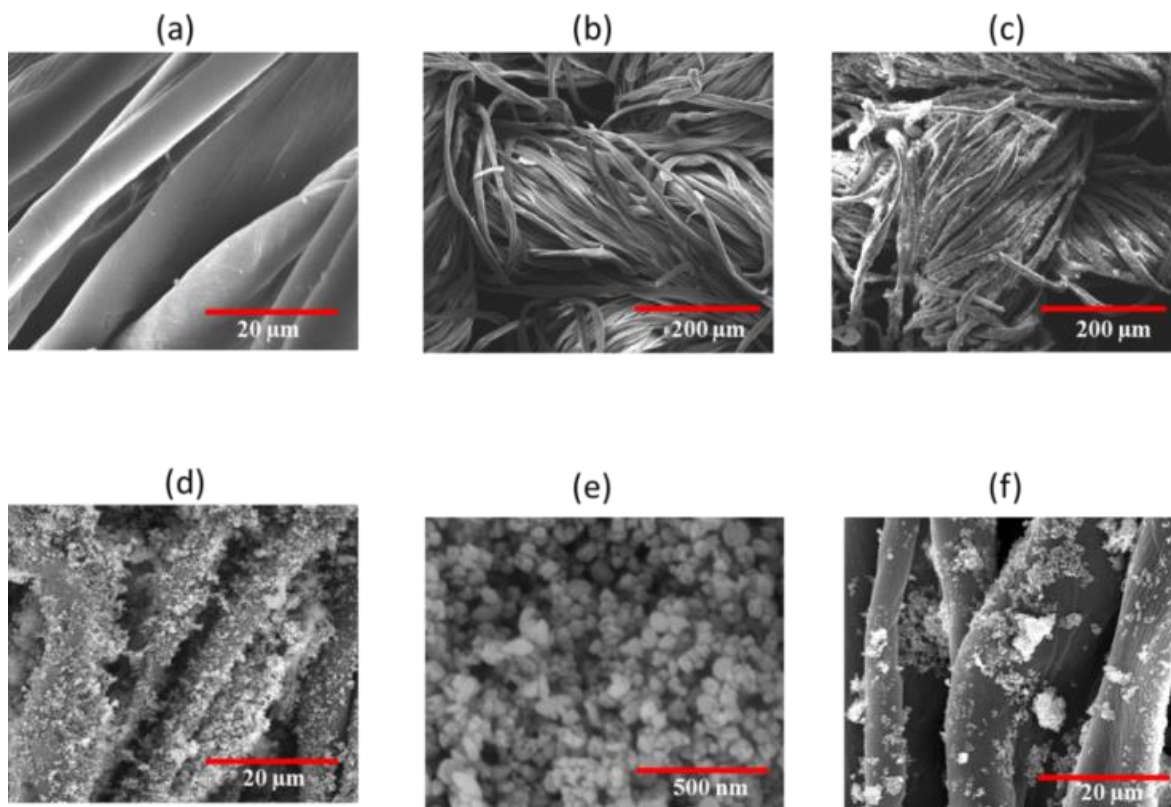


Figure 3. SEM images (a,b) pristine cotton, (c,d,e) sample 23 and (f) sample A.

5.3. Particle size

Figure 4 shows the particle size distribution of sonochemical in-situ synthesized ZnO NPs (optimized sample 23). It can be seen from Figure 4 that nanoparticle size distribution is uni-modal with an average particle size of 30.89 nm. At the nano scale the particles have increased surface areas, allowing the nanoparticles to be utilized in many technical applications [39], [40]. Dodd *et al.* reported that a decrease in particle size results in an augmentation of the specific surface area. Consequently, this augmentation also leads to an increase in the quantity of active surface sites. These sites facilitate the reaction between the photogenerated charge carriers and absorbed molecules, thereby giving rise to the formation of hydroxyl and superoxide radicals[41].

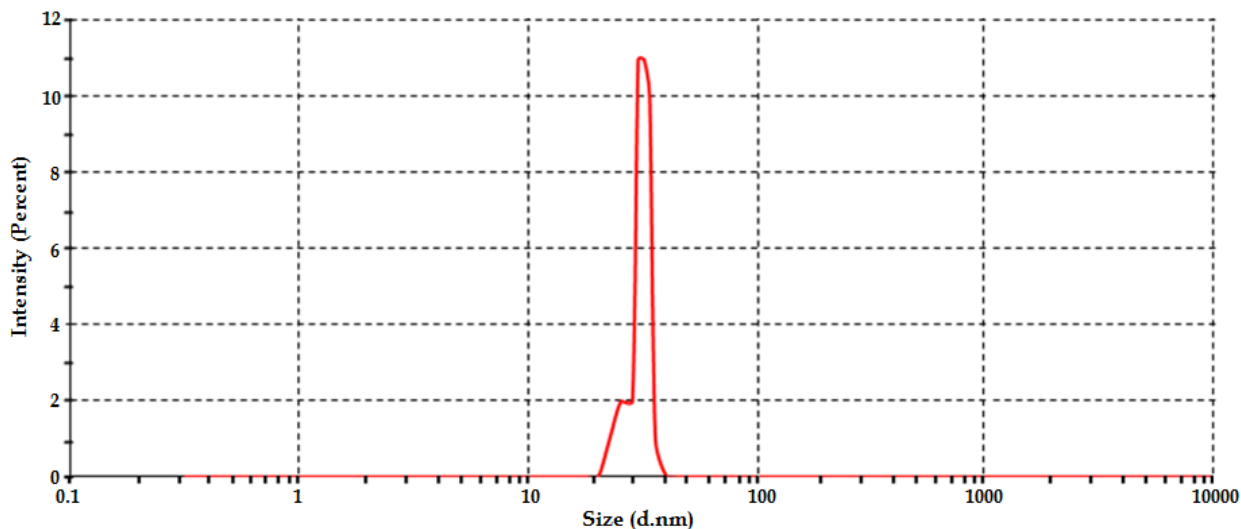


Figure 4. Particle size distribution sample 23.

5.4. XRD analysis

XRD diffractograms of pristine cotton fabric and optimized sonochemically treated sample 23 are presented in Figure 5. It is evident from Figure 5 that the pristine cotton fabric has only the characteristic peaks of cellulose (at $2\theta = 14.8, 16.5$ and 22.7) (JCDPS No.03-0226) [42]. While the sample 23 has some additional peaks (at $2\theta = 32.1, 34.7, 36.5, 47.8, 56.7, 63.1, 68.1, 69.2$) in the diffraction planes (100), (002), (101), (102), (110), (103), (200), and (112). These are characteristic peaks of ZnO NPs (as per diffraction standard No.36-1451 defined by the joint committee on powder diffraction standard (JCDPS)) [43]. The additional peaks are evidence of the presence of crystalline hexagonal wurtzite structure of ZnO NPs [44], [45]. The peak in plane (101) has the highest intensity, which shows that the (101) plane direction is the main dominant and leading growth direction for ZnO NPs. Moreover, in the case of sample 23, the peak intensity of the cellulose has decreased due to ZnO NPs loading. Furthermore, there is no extra peak in the diffractogram of sample 23 other than cellulose and ZnO NPs, which shows the purity of the ZnO NPs.

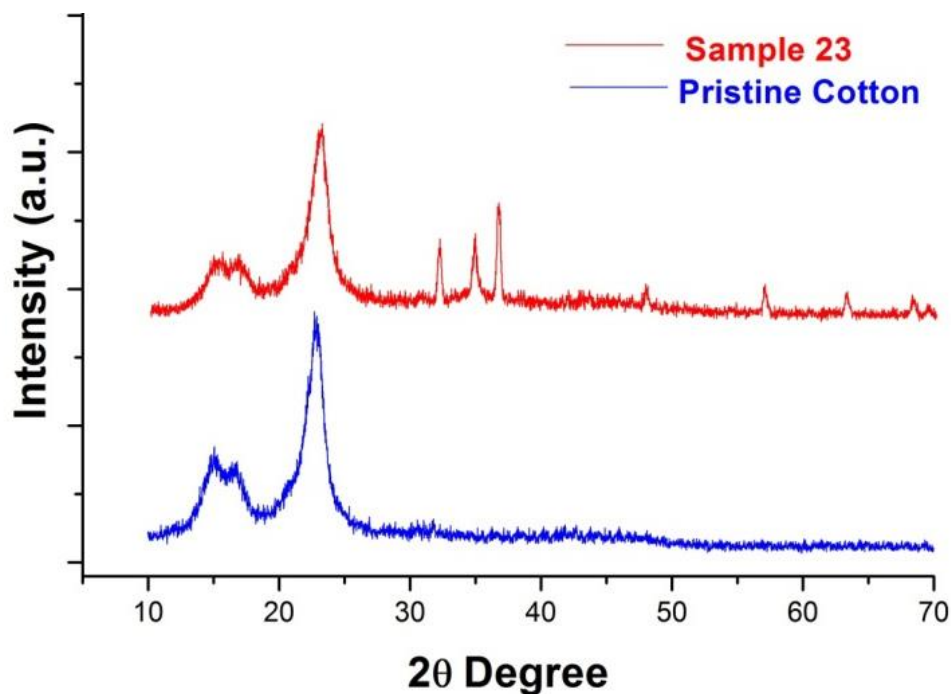


Figure 5. XRD diffractogram of pristine cotton and sample 23.

5.5. FTIR analysis

The FTIR spectra for pristine cotton, cotton-CA, sample 23, sample A, and sample B are presented in Figure 6. The pristine cotton has an O-H stretching band at 3300 cm^{-1} , which contains hydrogen bonding, a band at 2900 cm^{-1} is the result of C-H stretching, a band at 1310 cm^{-1} is due to the C-H wagging, while the peak at 1640 cm^{-1} shows the presence of absorbed H_2O molecules. The band at 1030 cm^{-1} was attributed to C=O stretching. The C-H bending is evident from the peak available at 1314 cm^{-1} [46], [47]. After citric acid treatment, a new absorption peak appeared at 1729 cm^{-1} , which can be attributed to the absorption of the carboxyl group from citric acid [48]. In the case of treated samples, there are some new peaks. The peak due to P=O is centered at 1250 cm^{-1} , while the peak centered at 884 cm^{-1} is associated with the P-O bond. Furthermore, the presence of the amide group can be confirmed by the peaks at 1624 cm^{-1} (amide vibration) and 1528 cm^{-1} (amide vibration), which are evidence of flame retardant treatment onto the cotton fabric [49]. Moreover, in the case of sample A and sample 23, there is a significant shift of FTIR spectra in the wavenumber range of 400 cm^{-1} to 500 cm^{-1} , which is attributed to the presence of ZnO NPs on the cotton fabric. In the case of sample 23, the intensity of spectra shift is more than that of sample A, which can be attributed to the high amount of ZnO NPs available in the case of sample 23. The shift of spectra in that wavenumber range can be attributed to the formation of the $-\text{CH}_2-\text{O}-\text{Zn}$ structure [45], [50].

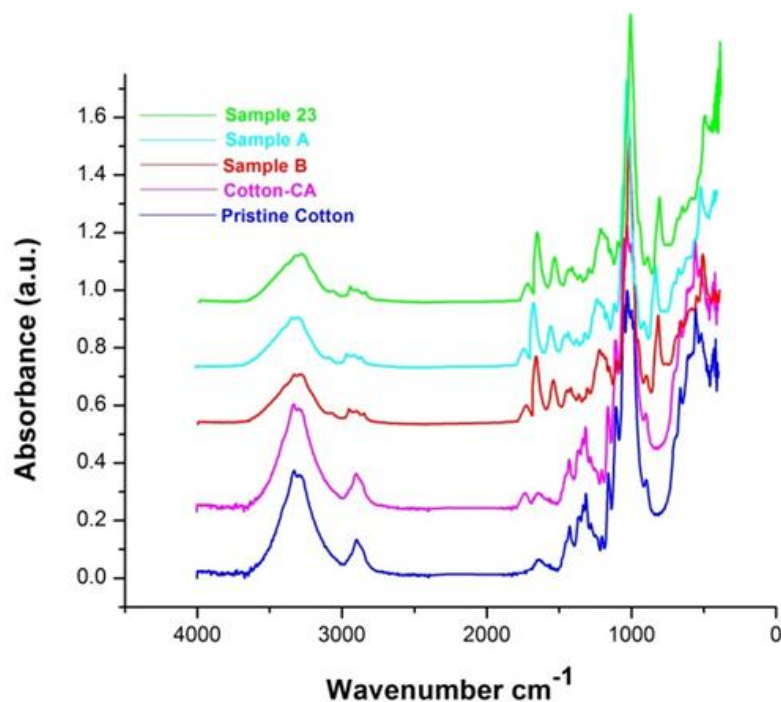


Figure 6. FTIR spectra of pristine cotton and sample A, sample B and sample 23.

5.6. Thermo gravimetric analysis

The thermal degradation trend of the fabric can be used to evaluate the flammability behavior of cotton fabric. So, the thermo gravimetric analysis of pristine cotton and developed samples was performed in a synthetic air environment. Figure 7(a) shows the weight loss percentage with the rise of temperature, Figure 7(b) shows the weight loss rate with the rise of temperature, whereas Table 3 shows the values of decomposition temperatures for pristine cotton and developed samples. In the case of the TGA curve for pristine cotton, there is only little weight loss below 343 °C, which corresponds to the evaporation of water molecules. In this region, the decarboxylation and dehydration process of cotton cellulose occurred, forming the aliphatic char and combustible gasses. The region 350 °C to 550 °C corresponds to the transformation of aliphatic char into an aromatic form of carbon dioxide and carbon monoxide [51]. Citric acid treated cotton fabric showed the same degradation behavior as pristine cotton but with little increase in residue. From Table 3, it can be seen that the $T_{\text{onset } 10\%}$ values have shifted towards lower temperatures after MDPA and ZnO NPs coating. For pristine cotton, $T_{\text{onset } 10\%}$ is 319.23 °C, while for sample 23, $T_{\text{onset } 10\%}$ is 266.07 °C, which is the lowest than all the samples. This attributes to the stronger performance of MDPA and ZnO NPs for the decomposition of cellulose as compared to pristine cotton. This T_{onset} mass loss is due to the evaporation of moisture contents from the fabric. Loading of MDPA and ZnO NPs tends to escalate the fabric's moisture, hence lowering the T_{onset} for developed samples than pristine cotton [52]. T_{max} for pristine cotton was observed at 343.15 °C, while after treatment, T_{max} decreased, and the lowest T_{max} was observed for sample 23 (i.e. 280.19 °C). From Table 3, it can be seen that the char residue at T_{max} and 600 °C increased after treatment compared to pristine cotton. This improvement can be explained as phosphorous components in MDPA were turned into phosphoric acid,

which caused the fabric's dehydration, hence leading to the lower degradation temperature and higher char residues [53]. The high char residual amount in the case of sample 23 corresponds to ZnO NPs [54]. The quantitative amount of char residue produced is associated with flame retardance performance [55]. The reduction in degradation temperature after MDPA treatment might be due to the fact that the O-P-C bond in MDPA is less stable than the C-O-C bond in cotton, and MDPA produced the phosphorous derivatives at lower temperature that might be accelerated cellulose degradation to char at lower temperature[56], [57]. While after ZnO NPs treatment, degradation temperature further decreased, which can be attributed to the loss of fiber strength during sonochemical process (will be discussed at next pages) which led to degradation of cellulose at lower temperature. The results are in accordance with Dhandapani *et al.* they also reported that ZnO NPs loaded cotton fabric during thermo gravimetric analysis showed lower degradation temperature and high char residue as compared to untreated cotton fabric [58]. In other study, Zhang *et al.* concluded that an increase in Zn contents on cellulosic fabric resulted as decrease of the degradation temperature and increase of char residues[11].

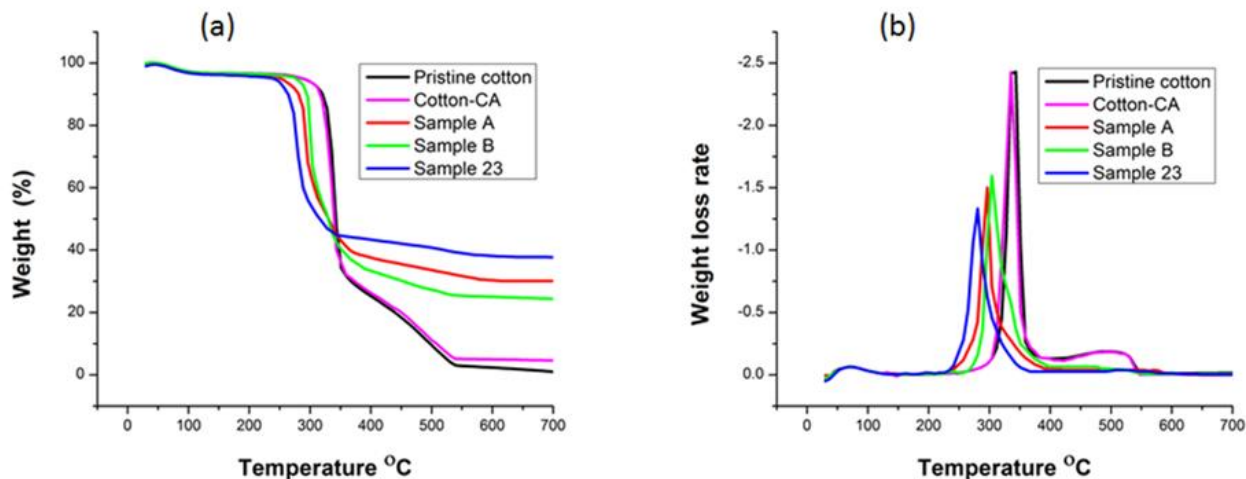


Figure 7. Thermo-oxidative behavior (a) TGA curves and (b) dTG curves.

Table 3. Thermal characteristics of pristine cotton and developed samples.

Sample	T _{onset 10%} (°C)	T _{max} (°C)	Residue at T _{max} (%)	Residue at 600 °C (%)
Pristine cotton	319.23	343.15	47.04	2.29
Cotton-CA	317.12	335.52	62.93	4.19
Sample A	280.34	296.13	68.47	30.91
Sample B	295.18	304.32	67.11	24.25
Sample 23	266.07	280.19	70.21	38.17

5.7. Vertical flame test

The measurements of the vertical flame test of untreated and developed samples are shown in Table 4 and Figure 8. It can be seen from Table 4 and Figure 8 that MDPA has a good effect on the flame retardancy of the cotton fabric, which further improved by the deposition of ZnO NPs.

It is evident from the results that flame retardant properties (i.e. after flame time, after glow time, char length) improved with increased deposition of ZnO NPs. The untreated sample burned intensely in contact with flame. After detaching the flame source, the burning process of the untreated sample remained continue until it completely burned out without any char formation. On the other hand, all the treated samples (MDPA treated and MDPA + ZnO NPs treated) were self-extinguished. Furthermore, char formation was observed in the case of treated samples (MDPA treated and MDPA + ZnO NPs treated). Moreover, it was observed that after flame time, after glow time, and char length of the treated samples decreased with an increased amount of Zn contents %. The best flame retardant results were observed in the case of sonochemically optimized sample 23. Sample 23 self-extinguished immediately after removal of the combustion source and had zero second after flame time, zero second after glow time, and 39 mm char length. Sample A developed by conventional magnetic stirring method had 2.13 seconds after flame time, zero second after glow time, and 76 mm char length, while sample B only treated with MDPA had 8.04 seconds after flame time, 5.21 seconds after glow time, and 127 mm char length. The char formation in the case of MDPA and MDPA + ZnO NPs treated samples was because of water removal from the fabric, the liberation of water leads to the dilution of the oxidizing gas phase, which created the insulating layer and protected the fabric after flame removal, hence increasing the flame retardancy [59]. Moreover, at elevated temperature phosphorous containing compounds release phosphate anions (pyro- and polyphosphates), these phosphate anions engage in char formation alongside the carbonized residues. This resulting carbonized layer known as char acts as a shield, effectively insulating and safeguarding the polymer from the flames while also impeding the diffusion of oxygen. Additionally, the presence of char hinders the volatilization of fuel and serves as a barrier against the generation of flammable free radicals [60], [61]. Phosphorus containing compounds are also capable of undergoing volatilization and into the gaseous state, thus leading to the creation of active radicals (such as $\text{PO}_2\cdot$, $\text{PO}\cdot$, and $\text{HPO}\cdot$) and serve as scavengers for $\text{H}\cdot$ and $\text{OH}\cdot$ radicals [60], [61]. Furthermore, ZnO NPs acted as co-catalyst and decreased the flame spread rate; therefore, improved flame retardancy was achieved [62]. A condensed phase mode of action through the heat barrier effect has been suggested as the foundation for flame retardancy of ZnO NPs [63].

Table 4. Experimental results for flammability test.

Sample	Zinc - acetate (M)	NaOH (M)	Sonication time (minutes)	MDPA (g/L)	Flammability test					
					After flame time		After glow time		Char length	
					(s)	Std. dev.	(s)	Std. dev.	(mm)	Std. dev.
Untreated	-	-	-	-	19.34	3.21	9.62	1.86	Completely burned	-
1	0.05	0.1	30	300	7.42	0.12	3.25	0.13	103	1.92
2	0.05	0.1	60	300	7.02	0.13	3.11	0.08	99	2.12
3	0.05	0.1	90	300	6.24	0.17	2.94	0.11	95	1.22
4	0.05	0.1	120	300	6.74	0.12	3.03	0.08	96	0.71
5	0.05	0.2	30	300	5.83	0.21	2.72	0.17	92	2.00
6	0.05	0.2	60	300	5.26	0.16	2.33	0.16	90	2.35
7	0.05	0.2	90	300	4.19	0.22	2.04	0.07	89	0.70
8	0.05	0.2	120	300	4.84	0.25	2.17	0.14	89	1.00
9	0.05	0.3	30	300	3.87	0.22	1.91	0.11	83	1.87
10	0.05	0.3	60	300	3.58	0.18	1.62	0.07	78	3.11
11	0.05	0.3	90	300	2.82	0.20	1.06	0.05	76	1.58
12	0.05	0.3	120	300	3.12	0.15	1.34	0.12	76	1.21
13	0.1	0.1	30	300	2.09	0.21	0.78	0.09	73	1.23
14	0.1	0.1	60	300	1.56	0.16	0.27	0.05	71	1.87
15	0.1	0.1	90	300	0.59	0.11	0	0	68	2.65
16	0.1	0.1	120	300	1.17	0.12	0	0	70	2.55
17	0.1	0.2	30	300	0	0	0	0	55	2.74
18	0.1	0.2	60	300	0	0	0	0	53	2.12
19	0.1	0.2	90	300	0	0	0	0	51	2.24
20	0.1	0.2	120	300	0	0	0	0	52	2.92
21	0.1	0.3	30	300	0	0	0	0	42	2.16
22	0.1	0.3	60	300	0	0	0	0	40	1.78
23	0.1	0.3	90	300	0	0	0	0	39	0.71
24	0.1	0.3	120	300	0	0	0	0	40	1.58
25	0.15	0.1	30	300	1.97	0.14	0.53	0.03	73	1.14
26	0.15	0.1	60	300	0.92	0.11	0	0	69	2.72
27	0.15	0.1	90	300	0.42	0.08	0	0	65	1.64
28	0.15	0.1	120	300	1.02	0.10	0	0	70	2.12
29	0.15	0.2	30	300	0	0	0	0	55	2.16
30	0.15	0.2	60	300	0	0	0	0	51	1.78
31	0.15	0.2	90	300	0	0	0	0	50	1.56
32	0.15	0.2	120	300	0	0	0	0	51	3.74
33	0.15	0.3	30	300	0	0	0	0	49	1.31
34	0.15	0.3	60	300	0	0	0	0	47	0.83
35	0.15	0.3	90	300	0	0	0	0	44	1.87
36	0.15	0.3	120	300	0	0	0	0	47	1.22
A	0.1	0.3	90 (magnetic stirring)	300	2.13	0.75	0	0	76	3.82
B	-	-	-	300	8.04	0.25	5.21	0.23	127	4.95

Wang *et al.* described that ZnO NPs could shield the insulating layer on the surface of the fiber, minimizing the amount of heat, fuel, and oxygen that are transferred from the flame to the fibers and, as a result, lowering the intensity as well as the rate of burning. Additionally, ZnO is already classified as a substance that suppresses the production of smoke [64]. Furthermore, these results are in accordance

with Samanta *et al.*, Wang *et al.*, and Arputharaj *et al.* they concluded that ZnO NPs greatly enhanced the amount of char residue, decreased the char length, and reduced the after flame time as well as afterglow time[64]–[66].

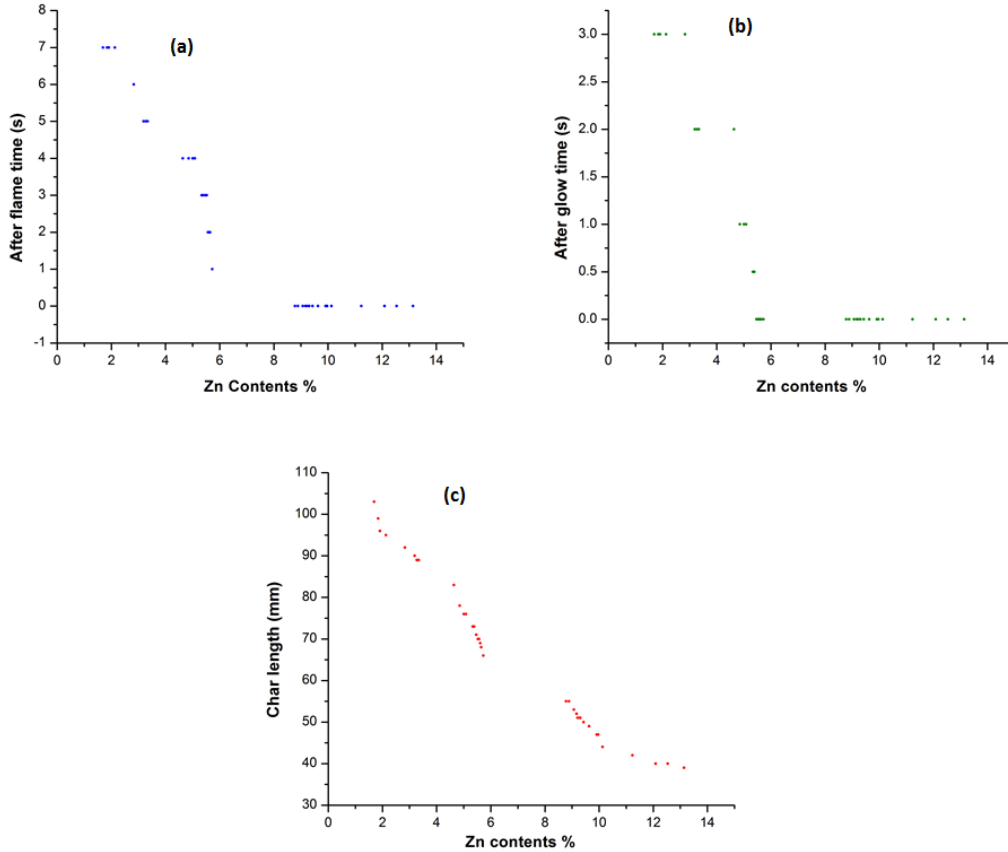


Figure 8. Flammability behavior (a) after flame time against Zn contents % (b) afterglow time against Zn contents % (c) char length against Zn contents %.

Equation (12) shows the regression model for prediction after flame time (s). The R-squared value presented in the model summary shows that the fitted model could explain 77.58 % of total variations , while p-value = 0.00 and F value = 99.78 presented in the model summary indicate that the model is significant.

$$\text{After flame time (s)} = 12.674 - 76.85 \text{ zinc acetate (M)} - 24.90 \text{ NaOH (M)} - 0.02118 \text{ sonication time (minutes)} + 121.2 \text{ zinc acetate (M)} \times \text{NaOH (M)} + 0.0724 \text{ zinc acetate (M)} \times \text{sonication time (minutes)} + 0.0383 \text{ NaOH (M)} \times \text{sonication time (minutes)} \quad (12)$$

Model summary of after flame time (s)

S = 1.17479 R-squared = 77.58% R-squared (adj) = 76.80% R-squared (pred) = 76.00% F-value = 99.78 p-value= 0.000

The regression model for predicting after glow time (s) is depicted by equation (13). The model summary displays the R-squared value, indicating that the fitted model can account for 76.93% of the total variations. Furthermore, the model summary presents the p-value as 0.00 and the F-value as 96.17, which suggest that the model is statistically significant.

$$\text{After glow time (s)} = 5.964 - 40.04 \text{ zinc acetate (M)} - 11.81 \text{ NaOH (M)} - 0.01032 \text{ sonication time (minutes)} + 73.4 \text{ zinc acetate (M)} \times \text{NaOH(M)} + 0.0383 \text{ zinc acetate (M)} \times \text{sonication time (minutes)} + 0.0153 \text{ NaOH (M)} \times \text{sonication time (minutes)} \quad (13)$$

Model summary of after glow time (s)

S = 0.556936 R-squared = 76.93% R-squared (adj) = 76.13% R-squared (pred) = 75.32 F-value = 96.17 p-value= 0.000

The regression model for predicting char length (mm) is demonstrated by equation (14). The model summary displays an R-squared value which indicates that the fitted model can account for 77.61% of the total variations. Furthermore, the model summary presents a p-value of 0.00 and an F-value of 97.40, both of which affirm that the model is statistically significant.

$$\text{Char length (mm)} = 127.05 - 319.5 \text{ zinc acetate (M)} - 112.8 \text{ NaOH (M)} - 0.0822 \text{ sonication time (minutes)} - 132 \text{ zinc acetate (M)} \times \text{NaOH (M)} + 0.231 \text{ zinc acetate (M)} \times \text{sonication time (minutes)} + 0.064 \text{ NaOH (M)} \times \text{sonication time (minutes)} \quad (14)$$

Model summary of char length (mm)

S = 9.29748 R-squared = 77.61% R-squared (adj) = 76.37% R-squared (pred) = 75.51% F-value = 97.40 p-value= 0.000

5.8. Limiting oxygen index (LOI)

LOI can be defined as the minimum available percentage amount of oxygen gas in the oxygen/nitrogen gas mixture that is necessary to continue the combustion process of a material [62]. As the LOI value of a material is increased it becomes more arduous to combustion. The LOI value of more than 27 indicates that the material is a flame retardant [62], [67]. Table 5 and Figure 9 show the values for LOI of treated and untreated fabric samples. It can be seen from Table 5 that the untreated sample has LOI value of 17.61, which indicates that pristine cotton is highly combustible. On the other hand, sample B; having flame retardant application, has LOI value of 23.81, which further increased after ZnO NPs application. Table 5 and Figure 9 show that the LOI value increased as the loaded concentration of ZnO NPs increased. These results are in accordance with Zhang *et al.* they concluded that the LOI value of cellulosic fibers increases as the loaded concentration of ZnO NPs increases [11]. The higher LOI value after ZnO NPs application might be due to the formation of a protective layer on fibers by ZnO NPs. The best LOI value was observed at 32.23 for sonochemically optimized sample 23. While, sample A, developed by the conventional magnetic stirring method, has the LOI value of 27.72, which is very near to the LOI value (27.42) of sample 27, which has less ZnO NPs concentration compared to sample A.

This might be due to the homogenous and smooth distribution of ZnO NPs in the case of sample 27 after the sonochemical process compared to the conventional magnetic stirring process.

Table 5. Experimental results for limiting oxygen index.

Sample	Zinc acetate (M)	NaOH (M)	Sonication time (minutes)	MDPA (g/L)	LOI	
					(%)	Std. dev.
Untreated	-	-	-	-	17.61	0.26
1	0.05	0.1	30	300	24.23	0.29
2	0.05	0.1	60	300	24.70	0.25
3	0.05	0.1	90	300	25.14	0.07
4	0.05	0.1	120	300	24.86	0.18
5	0.05	0.2	30	300	25.41	0.14
6	0.05	0.2	60	300	25.75	0.10
7	0.05	0.2	90	300	25.84	0.15
8	0.05	0.2	120	300	25.70	0.07
9	0.05	0.3	30	300	26.01	0.12
10	0.05	0.3	60	300	26.11	0.21
11	0.05	0.3	90	300	26.34	0.11
12	0.05	0.3	120	300	26.14	0.12
13	0.1	0.1	30	300	26.73	0.11
14	0.1	0.1	60	300	26.92	0.16
15	0.1	0.1	90	300	27.31	0.13
16	0.1	0.1	120	300	27.01	0.09
17	0.1	0.2	30	300	29.23	0.14
18	0.1	0.2	60	300	29.44	0.08
19	0.1	0.2	90	300	29.63	0.09
20	0.1	0.2	120	300	29.55	0.12
21	0.1	0.3	30	300	31.22	0.11
22	0.1	0.3	60	300	31.91	0.09
23	0.1	0.3	90	300	32.23	0.10
24	0.1	0.3	120	300	32.03	0.11
25	0.15	0.1	30	300	26.81	0.14
26	0.15	0.1	60	300	27.03	0.17
27	0.15	0.1	90	300	27.42	0.08
28	0.15	0.1	120	300	27.13	0.16
29	0.15	0.2	30	300	29.36	0.11
30	0.15	0.2	60	300	29.57	0.09
31	0.15	0.2	90	300	29.74	0.11
32	0.15	0.2	120	300	29.60	0.15
33	0.15	0.3	30	300	29.94	0.17
34	0.15	0.3	60	300	30.10	0.12
35	0.15	0.3	90	300	30.46	0.13
36	0.15	0.3	120	300	30.23	0.12
A	0.1	0.3	90 (magnetic stirring)	300	27.72	0.19
B	-	-	-	300	23.81	0.09

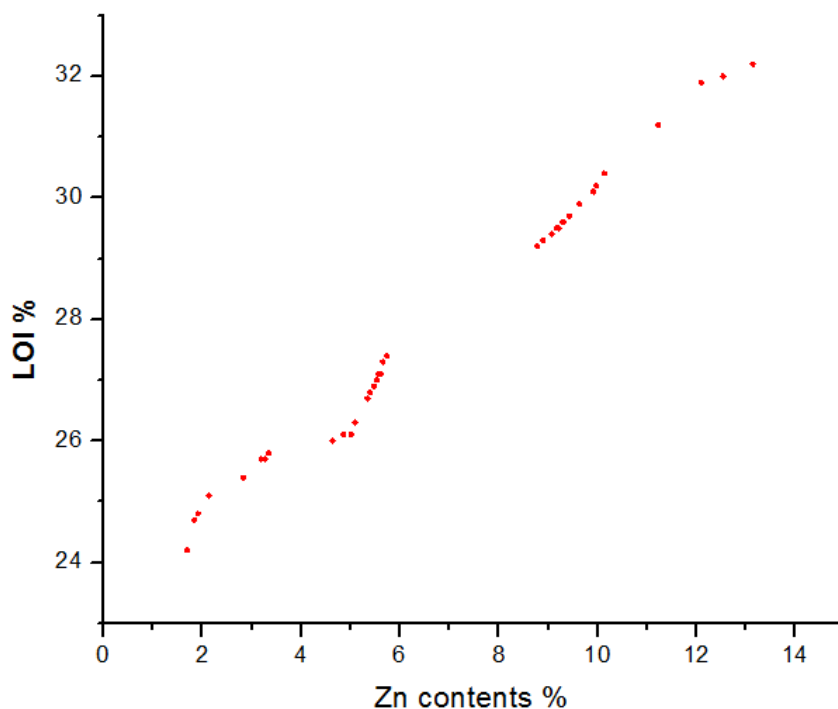


Figure 9. Graphical representation of LOI values vs Zn contents %.

The equation (15) shows the regression model for prediction of LOI %. R-squared value presented in model summary shows that the fitted model could explain 72.01 % of total variations , while p-value = 0.00 and F-value = 74.16 presented in model summary indicate that the model is significant.

$$\begin{aligned}
 LOI \% = & 22.633 + 17.97 \text{ zinc acetate } (M) + 7.55 \text{ NaOH } (M) + 0.00535 \text{ sonication time } (minutes) \\
 & + 82.0 \text{ zinc acetate } (M) \times \text{ NaOH}(M) - 0.0013 \text{ zinc acetate } (M) \times \text{ sonication time } (minutes) - \\
 & 0.0026 \text{ NaOH } (M) \times \text{ sonication time } (minutes) \quad (15)
 \end{aligned}$$

Model summary of LOI %

S = 1.21851 R-squared = 72.01% R-squared (adj) = 72.03% R-squared (pred) = 69.88 F-Value = 74.16 p-Value = 0.000

5.9. Antibacterial activity

Antibacterial activity of developed samples was investigated according to the colony count test procedure and shown in Table 6 and Figure 10. The results show that treated fabrics exhibit excellent bacterial reduction for both E.coli and S.aureus bacteria. From Table 6 and Figure 10, it is evident that

with an increased loaded amount of ZnO NPs, the antibacterial activity of the treated samples also increased for both E.coli and S.aureus bacteria. 100 % S.aureus reduction was achieved with 8.78 % loaded concentration of Zn contents (sample 17). While 100 % E.coli reduction was achieved with 9.07 % loaded concentration of Zn contents (sample 18). While the sample A developed by magnetic stirring showed 96.27% S.aureus reduction and 93.52% E.coli reduction. As the ZnO NPs interact with bacteria, they generate reactive oxygen species, such as H_2O_2 , $\bullet OH$, $\bullet O_2^-$. These reactive oxygen species damage the protein and DNA of the bacterial cell, resulting in the death of a bacterial cell. Furthermore, ZnO NPs deactivate the various necessary enzymes present in a bacterial cell; it is done by the interaction between the ZnO NPs and the thiol group present in bacterial cell. Moreover, the attachment of ZnO NPs onto the cell wall of the bacteria increase the Zn^{2+} cations concentration in the cytoplasm, which results in the death of bacteria [68], [69].

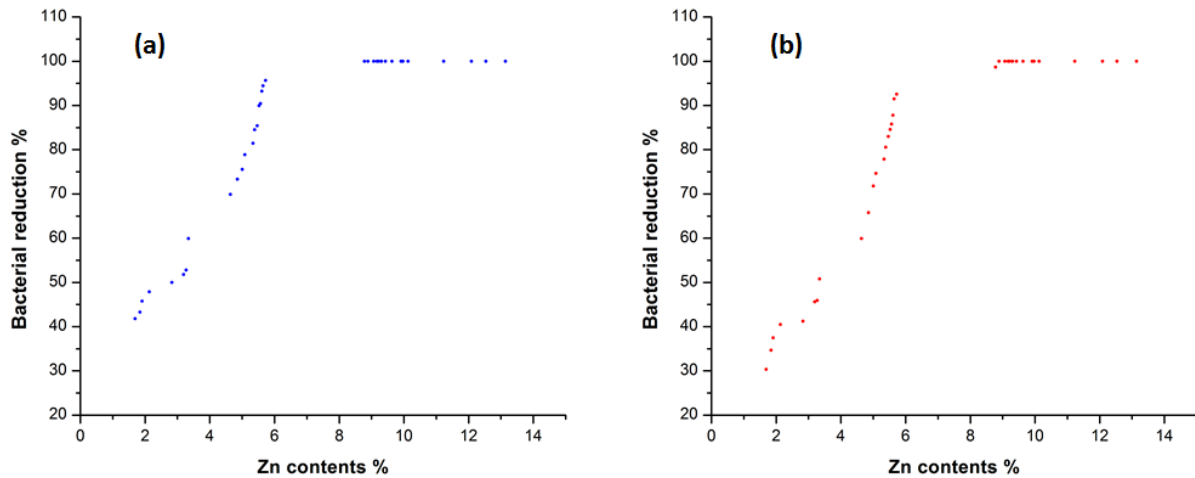


Figure 10. Graphical representation of antibacterial activity (a) S. aureus vs Zn contents % (b) E. coli vs Zn contents %.

The regression model for predicting the S.aureus bacterial reduction % is displayed in equation (16). The fitted model could explain 76.71% of the total changes, according to the R-squared value provided in the model summary. The model is significant, as indicated by the p-value of 0.00 and the F-value of 94.95 presented in the model summary.

$$S. aureus \text{ bacterial reduction } \% = - 3.63 + 630.3 \text{ zinc acetate } (M) + 208.6 \text{ NaOH } (M) + 0.1341 \text{ sonication time (minutes)} - 1034 \text{ zinc acetate } (M) \times \text{NaOH } (M) - 0.392 \text{ zinc acetate } (M) \times \text{sonication time (minutes)} - 0.271 \text{NaOH } (M) \times \text{sonication time (minutes)} \quad (16)$$

Model summary of *S.aureus* bacterial reduction %

S = 10.0808 R-squared = 76.71% R-squared (adj) = 75.90% R-squared (pred) = 75.14% F-Value = 94.95 p-Value = 0.000

Table 6. Experimental results for antibacterial activity.

Sample	Zinc acetate (M)	NaOH (M)	Sonication time (minutes)	MDPA (g/L)	Bacterial reduction %			
					S. aureus		E.coli	
					R (%)	Std. dev.	R (%)	Std. dev.
1	0.05	0.1	30	300	41.78	3.44	30.34	3.37
2	0.05	0.1	60	300	43.29	3.52	34.67	4.53
3	0.05	0.1	90	300	47.86	3.72	40.45	3.42
4	0.05	0.1	120	300	45.76	4.21	37.47	4.50
5	0.05	0.2	30	300	49.97	5.53	41.23	5.05
6	0.05	0.2	60	300	51.79	4.44	45.57	3.76
7	0.05	0.2	90	300	59.93	3.76	50.78	4.03
8	0.05	0.2	120	300	52.79	5.96	45.91	2.48
9	0.05	0.3	30	300	69.86	4.75	59.92	3.62
10	0.05	0.3	60	300	73.32	3.72	65.76	3.30
11	0.05	0.3	90	300	78.84	4.30	74.65	2.73
12	0.05	0.3	120	300	75.54	4.32	71.78	2.15
13	0.1	0.1	30	300	81.45	3.41	77.87	2.16
14	0.1	0.1	60	300	85.42	4.03	82.98	3.31
15	0.1	0.1	90	300	94.43	1.60	91.46	4.32
16	0.1	0.1	120	300	89.95	2.14	84.56	2.68
17	0.1	0.2	30	300	100	0	98.64	0.86
18	0.1	0.2	60	300	100	0	100	0
19	0.1	0.2	90	300	100	0	100	0
20	0.1	0.2	120	300	100	0	100	0
21	0.1	0.3	30	300	100	0	100	0
22	0.1	0.3	60	300	100	0	100	0
23	0.1	0.3	90	300	100	0	100	0
24	0.1	0.3	120	300	100	0	100	0
25	0.15	0.1	30	300	84.49	2.59	80.54	2.17
26	0.15	0.1	60	300	93.23	2.10	87.76	2.33
27	0.15	0.1	90	300	95.67	1.37	92.51	2.31
28	0.15	0.1	120	300	90.42	2.40	85.78	1.63
29	0.15	0.2	30	300	100	0	100	0
30	0.15	0.2	60	300	100	0	100	0
31	0.15	0.2	90	300	100	0	100	0
32	0.15	0.2	120	300	100	0	100	0
33	0.15	0.3	30	300	100	0	100	0
34	0.15	0.3	60	300	100	0	100	0
35	0.15	0.3	90	300	100	0	100	0
36	0.15	0.3	120	300	100	0	100	0
A	0.1	0.3	90 (magnetic stirring)	300	96.27	3.35	93.52	4.67

Equation (17) shows the regression model for forecasting the E. coli bacterial reduction %. The R-squared value in the model summary indicates that 76.84% of the total changes could be explained by the fitted model. The model is significant, as shown by the model summary's F-value of 95.65 and p-value of 0.00.

$$E. coli bacterial reduction \% = -17.56 + 704.6 \text{ zinc acetate } (M) + 210.2 \text{ NaOH } (M) + 0.1671 \text{ sonication time } (minutes) - 946 \text{ zinc acetate } (M) \times \text{ NaOH } (M) - 0.784 \text{ zinc acetate } (M) \times \text{ sonication time } (minutes) - 0.177 \text{ NaOH } (M) \times \text{ sonication time } (minutes) \quad (17)$$

Model summary of E.coli reduction %

S = 11.6385 R-squared = 76.84% R-squared (adj) = 76.03% R-squared (pred) = 75.29% F-Value = 95.65 p-Value = 0.000

5.10. Ultraviolet protection factor (UPF)

The UV protection factors (UPF values) of the untreated and developed samples are shown in Table 7 and Figure 11. It is apparent from Table 7 and Figure 11 that untreated cotton fabric has an UPF value of 4.78, while the UPF value of sonochemically synthesized optimized sample 23 has 143.76. It can also be seen from Table 7 and Figure 11 that with the increase in ZnO NPs concentration, the UPF values of the samples also increase. The study by Han and Yu supports these results; they concluded that the UV blocking ability of textile material increases with increasing the metal oxide amount in the textile matrix [70]. The higher UPF value indicates that the fabric has a higher ability to protect against UV radiations [71]. ZnO NPs have a high refractive index, which causes the UV radiations to be scattered when they interact with ZnO NPs, and not to be transmitted to the human body [72]. Furthermore, when exposed to UV rays, ZnO NPs absorb the corresponding energy through the interaction with their electrons, impeding the penetration of such radiation from the fabric into the skin. This absorption phenomenon plays a pivotal role in safeguarding the integrity of DNA within skin cells, thereby reducing the likelihood of both sunburn and long-lasting skin harm [73], [74]. Apart from absorption, ZnO NPs exhibit reflective attributes within the UV range, effectively deflecting a proportion of the incident UV radiation away from the surface of the fabric [73]. This reflective mechanism imparts an additional layer of protection against harmful UV exposure.

Table 7 shows that the sample A with 7.83 % ZnO NPs concentration has a 52.05 UPF value, and sample 27 with 5.73 % ZnO NPs has a 50.96 UPF value; the high difference in ZnO NPs concentrations and very little difference in UPF values of these samples can be explained as better and smooth distribution of ZnO NPs in case of sample 27 by the sonochemical process as compared to sample A which is prepared by the conventional stirring method.

Table 7. Experimental results for UV protection.

Sample	Zinc acetate (M)	NaOH (M)	Sonication time (minutes)	MDPA (g/L)	UV protection	
					UPF	Std. dev.
Untreated	-	-	-	-	4.78	0.11
1	0.05	0.1	30	300	19.12	0.50
2	0.05	0.1	60	300	20.31	0.36
3	0.05	0.1	90	300	20.87	0.25
4	0.05	0.1	120	300	20.64	0.14
5	0.05	0.2	30	300	20.94	0.33
6	0.05	0.2	60	300	21.53	0.39
7	0.05	0.2	90	300	21.72	0.24
8	0.05	0.2	120	300	21.67	0.35
9	0.05	0.3	30	300	32.52	0.41
10	0.05	0.3	60	300	33.71	0.29
11	0.05	0.3	90	300	34.13	0.20
12	0.05	0.3	120	300	33.98	0.24
13	0.1	0.1	30	300	34.39	0.23
14	0.1	0.1	60	300	37.17	0.37
15	0.1	0.1	90	300	49.09	1.58
16	0.1	0.1	120	300	37.98	0.90
17	0.1	0.2	30	300	67.74	1.10
18	0.1	0.2	60	300	73.89	1.62
19	0.1	0.2	90	300	93.34	2.46
20	0.1	0.2	120	300	82.98	2.61
21	0.1	0.3	30	300	134.32	3.18
22	0.1	0.3	60	300	134.87	2.77
23	0.1	0.3	90	300	143.76	3.43
24	0.1	0.3	120	300	139.93	2.64
25	0.15	0.1	30	300	36.89	0.58
26	0.15	0.1	60	300	48.04	1.03
27	0.15	0.1	90	300	50.96	1.45
28	0.15	0.1	120	300	42.74	1.21
29	0.15	0.2	30	300	71.87	1.09
30	0.15	0.2	60	300	84.45	1.46
31	0.15	0.2	90	300	97.12	3.99
32	0.15	0.2	120	300	87.92	2.03
33	0.15	0.3	30	300	104.45	2.27
34	0.15	0.3	60	300	111.56	3.07
35	0.15	0.3	90	300	124.47	5.08
36	0.15	0.3	120	300	121.34	2.71
A	0.1	0.3	90 (magnetic stirring)	300	52.05	6.09
B	-	-	-	300	13.23	0.26

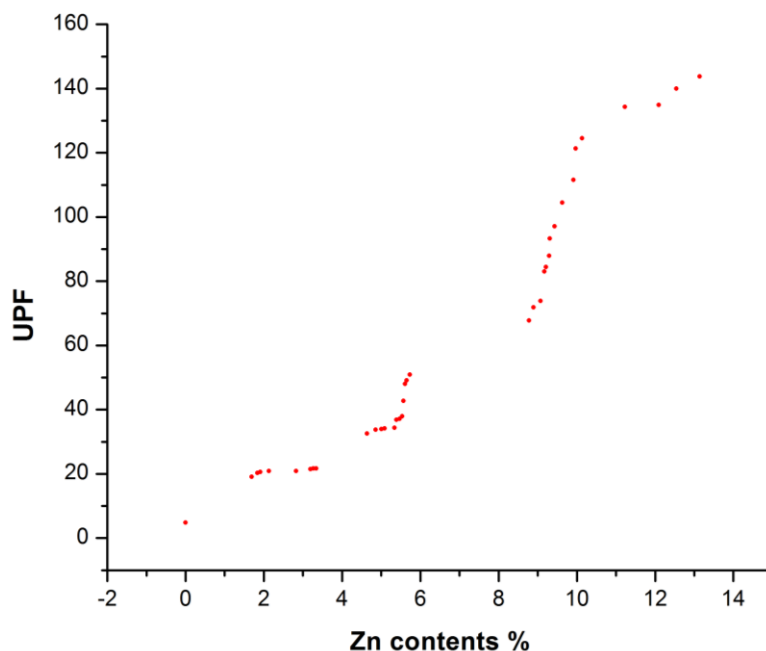


Figure 11. Graphical representation of UPF values against Zn contents %.

Equation (18) shows the regression model for the prediction of UPF value. The R-squared value presented in the model summary shows that the fitted model could explain 76.70 % of total variations , while p-value = 0.00 and F-value = 94.90 presented in the model summary indicate that the model is significant.

$$UPF = 11.4 - 117 \text{ zinc acetate } (M) - 1.8 \text{ NaOH } (M) - 0.098 \text{ sonication time } (minutes) + 2872 \text{ zinc acetate } (M) \times \text{NaOH } (M) + 1.47 \text{ zinc acetate } (M) \times \text{sonication time } (minutes) + 0.256 \text{ NaOH } (M) \times \text{sonication time } (minutes) \quad (18)$$

Model summary of UPF

S = 19.973 R-squared = 76.70% R-squared (adj) = 75.89% R-squared (pred) = 74.98% F-value = 94.90 p-value = 0.000

5.11. Self-cleaning

Cotton fabrics coated with ZnO NPs and MDPA were analyzed for self-cleaning using photocatalytic degradation of coffee stain under 8 hours of UV irradiation. Figure 13 shows the scanned images of samples before and after UV irradiation. Table 8 shows the color intensity of samples after 8 hours of UV irradiation time. In image J software black has 0 color intensity while white has 255, so greater the

value of color intensity, the more the color towards the white. Figure 12 shows the relation between Zn contents % and color intensity. It is clear that color intensity increases with the increase of the loaded amount of Zn contents. Untreated sample after 8 hours of UV irradiation time has color intensity 150.51. Sample A and sample B have color intensity 214.88 and 151.42 respectively. The higher color intensity of sample A than sample B is due to the presence of ZnO NPs at the surface of fabric[23]. Sample 23 showed the excellent results having color intensity of 250.27, which is very near to the color intensity value of white color. These results are in line with Sudrajat. H work demonstrating that the higher photo catalytic activity is obtained at higher amounts of ZnO NPs[75]. When ZnO NPs exist on the top of textile fabrics, ZnO NPs has the ability to react and degrade different organic dirt stains, both colorful and colorless[76]. As compared to untreated cotton fabric, the higher photo catalytic activity of ZnO NPs loaded cotton fabrics is because of ZnO NPs on the surface of the cotton fabrics, since ZnO NPs cause degradation of the dye molecules by photo catalytic reactions[77]. In the photo-catalytic mechanism by ZnO NPs, two photochemical reactions “oxidation and reduction” occur. During these reactions reactive oxygen species “ $\bullet\text{OH}$ and $\bullet\text{O}_2$ ” are produced. The $\bullet\text{OH}$ radical has a vital role in oxidating the dye molecules[73].

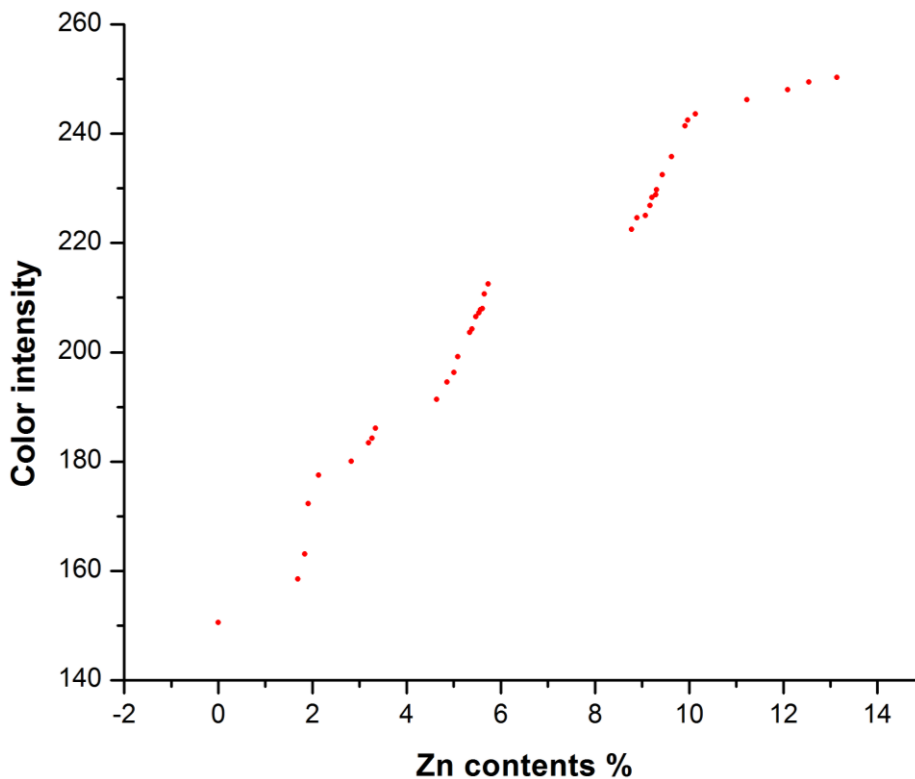


Figure 12. Graphical representation of color intensity against Zn contents %.

Table 8. Experimental results for self-cleaning.

Sample	Zinc acetate (M)	NaOH (M)	Sonication time (minutes)	MDPA (g/L)	Self-cleaning	
					Color Intensity	Std. dev.
Untreated	-	-	-	-	150.51	1.47
1	0.05	0.1	30	300	158.53	3.91
2	0.05	0.1	60	300	163.05	3.21
3	0.05	0.1	90	300	177.53	2.46
4	0.05	0.1	120	300	172.29	3.31
5	0.05	0.2	30	300	180.02	4.12
6	0.05	0.2	60	300	183.41	3.14
7	0.05	0.2	90	300	186.13	2.26
8	0.05	0.2	120	300	184.29	3.30
9	0.05	0.3	30	300	191.34	2.24
10	0.05	0.3	60	300	194.51	3.24
11	0.05	0.3	90	300	199.20	4.77
12	0.05	0.3	120	300	196.27	3.62
13	0.1	0.1	30	300	203.62	4.01
14	0.1	0.1	60	300	206.54	2.58
15	0.1	0.1	90	300	210.63	3.25
16	0.1	0.1	120	300	207.19	2.91
17	0.1	0.2	30	300	222.51	4.37
18	0.1	0.2	60	300	225.05	5.58
19	0.1	0.2	90	300	229.71	3.41
20	0.1	0.2	120	300	226.86	3.29
21	0.1	0.3	30	300	246.24	1.34
22	0.1	0.3	60	300	248.06	1.01
23	0.1	0.3	90	300	250.27	1.04
24	0.1	0.3	120	300	249.49	1.29
25	0.15	0.1	30	300	204.29	4.18
26	0.15	0.1	60	300	207.97	3.80
27	0.15	0.1	90	300	212.51	2.93
28	0.15	0.1	120	300	207.80	3.84
29	0.15	0.2	30	300	224.62	6.24
30	0.15	0.2	60	300	228.35	3.77
31	0.15	0.2	90	300	232.50	3.74
32	0.15	0.2	120	300	228.83	2.81
33	0.15	0.3	30	300	235.77	3.67
34	0.15	0.3	60	300	241.46	3.76
35	0.15	0.3	90	300	243.61	1.36
36	0.15	0.3	120	300	242.47	3.42
A	0.1	0.3	90 (magnetic stirring)	300	214.88	4.53
B	-	-	-	300	151.42	1.32

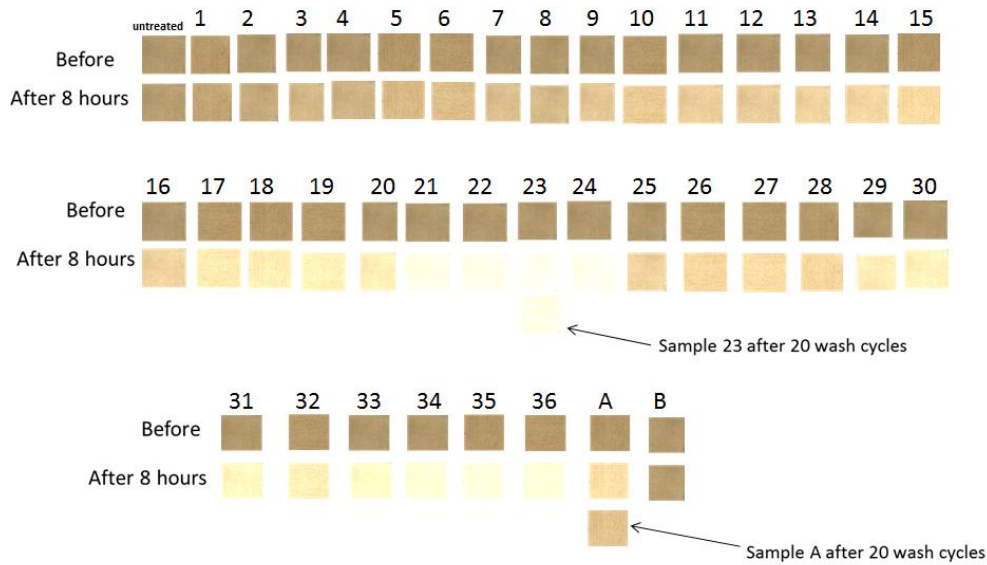


Figure 13. Degradation of coffee stain under UV-visible light irradiation.

The regression model for predicting color intensity is depicted by equation (19). The model summary displays the R-squared value, indicating that the fitted model can account for 78.49% of the total variations. Furthermore, the model summary presents the p-value as 0.00 and the F-value as 105.21, which suggests that the model is statistically significant.

$$Color\ intensity = 128.44 + 414.9\ zinc\ acetate\ (M) + 156.8\ NaOH\ (M) + 0.1464\ sonication\ time\ (minutes) + 260\ zinc\ acetate\ (M) \times NaOH\ (M) - 0.407\ zinc\ acetate\ (M) \times sonication\ time\ (minutes) - 0.178\ NaOH\ (M) \times sonication\ time\ (minutes) \quad (19)$$

Model summary of color intensity

S = 12.125 R-squared = 78.49% R-squared (adj) = 77.74% R-squared (pred) = 76.85% F-value = 105.21 p-value = 0.000

5.12. Bending rigidity

Bending rigidity or stiffness is an important property of fabric which further influences fabric draping and wrinkling behavior. Each sample with a 50mm width was clamped in the instrument from one side while the other side drove through the sensor jaws, as shown in Figure 14. The measurement of each sample was repeated five times. The average bending force was obtained for each sample, and with the help of bending force the bending rigidity was calculated by using equation (20)[78].

$$B = k \cdot Fm \quad (20)$$

Where B is bending rigidity

k is constant and $k= 0.7 \times 10^{-6}$

Fm is bending force



Figure 14. Bending Tester TH-7.

The measured values of bending force and bending rigidity are tabulated in Table 9. While Figure 15 shows the plot of bending force against Zn contents %. It is obvious from Table 9 that after MDPA coating the bending force and as well as bending rigidity of the fabric in both warp wise and weft wise directions are increased. From the results shown in Table 9 it is clear that after ZnO NPs coating the bending force and bending rigidity is further increased in both directions. Untreated fabric has warp wise and weft wise bending rigidity as 0.0581×10^{-4} Nm and 0.0392×10^{-4} Nm, respectively. While the sample B only coated with flame retardant chemical has warp wise bending rigidity 0.0787×10^{-4} Nm and weft wise bending rigidity 0.0501×10^{-4} Nm. The highest bending rigidity was recorded for sample 23 with highest amount of ZnO NPs as 0.0969×10^{-4} Nm and 0.0612×10^{-4} Nm warp wise and weft wise respectively. Figure 15 shows that with the increased amount of ZnO NPs deposition on to the fabric the bending force to bend the fabric also increased. The increase in bending force with the increase of ZnO NPs is also reported by Khan *et al.* They concluded that bending force and stiffness of the fabric have a linear increasing relationship with amount and size of ZnO nano rods[79]. In one more study, Tania and Ali also reported increase in stiffness of the cotton fabric after ZnO NPs deposition on to the cotton fabric[80].

Table 9. Experimental results for bending rigidity.

Sample	Zinc acetate (M)	NaOH (M)	Sonication time (minutes)	MDPA (g/L)	Bending force (Fm) (mN)				Bending rigidity (B) (Nm)	
					Warp wise	Std. dev.	Weft wise	Std. dev.	Warp wise	Weft wise
Untreated	-	-	-	-	8.314	0.017	5.278	0.008	0.0581×10 ⁻⁴	0.0392×10 ⁻⁴
1	0.05	0.1	30	300	11.328	0.031	7.206	0.018	0.0792×10 ⁻⁴	0.0504×10 ⁻⁴
2	0.05	0.1	60	300	11.352	0.018	7.218	0.019	0.0794×10 ⁻⁴	0.0505×10 ⁻⁴
3	0.05	0.1	90	300	11.412	0.017	7.250	0.016	0.0798×10 ⁻⁴	0.0507×10 ⁻⁴
4	0.05	0.1	120	300	11.368	0.022	7.228	0.013	0.0795×10 ⁻⁴	0.0506×10 ⁻⁴
5	0.05	0.2	30	300	11.466	0.020	7.294	0.023	0.0802×10 ⁻⁴	0.0510×10 ⁻⁴
6	0.05	0.2	60	300	11.526	0.023	7.322	0.016	0.0806×10 ⁻⁴	0.0512×10 ⁻⁴
7	0.05	0.2	90	300	11.592	0.016	7.366	0.019	0.0811×10 ⁻⁴	0.0515×10 ⁻⁴
8	0.05	0.2	120	300	11.558	0.014	7.340	0.015	0.0809×10 ⁻⁴	0.0513×10 ⁻⁴
9	0.05	0.3	30	300	11.730	0.020	7.452	0.019	0.0821×10 ⁻⁴	0.0521×10 ⁻⁴
10	0.05	0.3	60	300	11.772	0.022	7.486	0.020	0.0824×10 ⁻⁴	0.0524×10 ⁻⁴
11	0.05	0.3	90	300	11.824	0.018	7.510	0.015	0.0827×10 ⁻⁴	0.0526×10 ⁻⁴
12	0.05	0.3	120	300	11.801	0.023	7.502	0.019	0.0826×10 ⁻⁴	0.0525×10 ⁻⁴
13	0.1	0.1	30	300	11.860	0.025	7.532	0.013	0.0830×10 ⁻⁴	0.0527×10 ⁻⁴
14	0.1	0.1	60	300	11.918	0.019	7.560	0.016	0.0834×10 ⁻⁴	0.0529×10 ⁻⁴
15	0.1	0.1	90	300	12.014	0.021	7.628	0.013	0.0841×10 ⁻⁴	0.0533×10 ⁻⁴
16	0.1	0.1	120	300	11.945	0.018	7.584	0.021	0.0836×10 ⁻⁴	0.0531×10 ⁻⁴
17	0.1	0.2	30	300	12.630	0.026	7.992	0.019	0.0841×10 ⁻⁴	0.0559×10 ⁻⁴
18	0.1	0.2	60	300	12.741	0.023	8.062	0.019	0.0892×10 ⁻⁴	0.0564×10 ⁻⁴
19	0.1	0.2	90	300	12.842	0.028	8.132	0.013	0.0899×10 ⁻⁴	0.0569×10 ⁻⁴
20	0.1	0.2	120	300	12.782	0.026	8.094	0.018	0.0895×10 ⁻⁴	0.0566×10 ⁻⁴
21	0.1	0.3	30	300	13.322	0.022	8.428	0.019	0.0932×10 ⁻⁴	0.0589×10 ⁻⁴
22	0.1	0.3	60	300	13.524	0.027	8.546	0.018	0.0947×10 ⁻⁴	0.0598×10 ⁻⁴
23	0.1	0.3	90	300	13.848	0.035	8.756	0.016	0.0969×10 ⁻⁴	0.0612×10 ⁻⁴
24	0.1	0.3	120	300	13.640	0.025	8.614	0.021	0.0954×10 ⁻⁴	0.0603×10 ⁻⁴
25	0.15	0.1	30	300	11.882	0.028	7.548	0.017	0.0832×10 ⁻⁴	0.0528×10 ⁻⁴
26	0.15	0.1	60	300	11.988	0.018	7.616	0.018	0.0839×10 ⁻⁴	0.0533×10 ⁻⁴
27	0.15	0.1	90	300	12.042	0.019	7.640	0.016	0.0843×10 ⁻⁴	0.0535×10 ⁻⁴
28	0.15	0.1	120	300	11.960	0.018	7.596	0.025	0.0837×10 ⁻⁴	0.0532×10 ⁻⁴
29	0.15	0.2	30	300	12.694	0.029	8.034	0.018	0.0889×10 ⁻⁴	0.0562×10 ⁻⁴
30	0.15	0.2	60	300	12.804	0.025	8.108	0.014	0.0896×10 ⁻⁴	0.0567×10 ⁻⁴
31	0.15	0.2	90	300	12.874	0.038	8.150	0.016	0.0901×10 ⁻⁴	0.0570×10 ⁻⁴
32	0.15	0.2	120	300	12.836	0.027	8.124	0.015	0.0898×10 ⁻⁴	0.0568×10 ⁻⁴
33	0.15	0.3	30	300	12.912	0.024	8.164	0.018	0.0904×10 ⁻⁴	0.0571×10 ⁻⁴
34	0.15	0.3	60	300	13.008	0.019	8.234	0.015	0.0910×10 ⁻⁴	0.0576×10 ⁻⁴
35	0.15	0.3	90	300	13.114	0.024	8.292	0.017	0.0918×10 ⁻⁴	0.0580×10 ⁻⁴
36	0.15	0.3	120	300	13.048	0.027	8.248	0.013	0.0913×10 ⁻⁴	0.0577×10 ⁻⁴
A	0.1	0.3	90 (magnetic stirring)	300	12.431	0.036	7.824	0.021	0.0870×10 ⁻⁴	0.0548×10 ⁻⁴
B	-	-	-	300	11.246	0.023	7.146	0.011	0.0787×10 ⁻⁴	0.0501×10 ⁻⁴

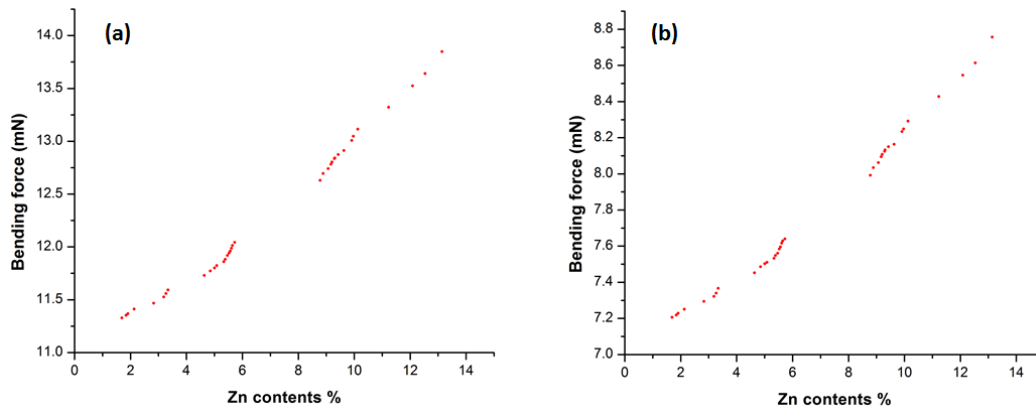


Figure 15. Graphical representation of bending force against Zn contents % (a) warp wise (b) weft wise.

Equations (21) and (22) show the regression model used to determine bending force warp wise and weft wise respectively. According to the model summary, for warp wise bending force the fitted model can explain 72.18% of the total variances based on its R-squared value. Furthermore, the model summary for warp wise bending force indicates the model's significance with a p-value of 0.000 and an F-value of 74.81. According to the model summary, for weft wise bending force the fitted model can explain 71.96% of the total variances based on its R-squared value. Furthermore, the model summary for weft wise bending force indicates the model's significance with a p-value of 0.000 and an F-value of 74.00.

$$\text{Bending force (mN) (warp wise)} = 10.892 + 3.57 \text{ zinc acetate (M)} + 1.50 \text{ NaOH (M)} - 0.00037 \text{ sonication time (minutes)} + 31.80 \text{ zinc acetate (M)} \times \text{NaOH (M)} + 0.0057 \text{ zinc acetate (M)} \times \text{sonication time (minutes)} + 0.0069 \text{ NaOH (M)} \times \text{sonication time (minutes)} \quad (21)$$

Model summary for bending force warp wise

S = 0.387 R-squared = 72.18% R-squared (adj) = 71.22% R-squared (pred) = 70.15% F-value = 74.81 p-value = 0.00

$$\text{Bending force (mN) (weft wise)} = 6.926 + 2.31 \text{ zinc acetate (M)} + 0.998 \text{ NaOH (M)} - 0.00025 \text{ sonication time (minutes)} + 18.62 \text{ zinc acetate (M)} \times \text{NaOH (M)} + 0.0037 \text{ zinc acetate (M)} \times \text{sonication time (minutes)} + 0.00423 \text{ NaOH (M)} \times \text{sonication time (minutes)} \quad (22)$$

Model summary for bending force weft wise

S = 0.237 R-squared = 71.96% R-squared (adj) = 70.99% R-squared (pred) = 69.91% F-value = 74.00 p-value = 0.000

5.13. Air permeability

The air permeability of a fabric is dependent on factors such as its porosity, cross-section, shape of the fabric, and number of channels. Additionally, the thermal properties of the fabric are primarily influenced by its air permeability[81]. The air permeability of textile fabrics holds significance as a comfort attribute. Moreover, it is crucial to examine the impact of coating on the fabric's air permeation. Table 10 shows the results for air permeability of the untreated and treated samples. While the Figure 16 shows the relation between the synthesized amount of ZnO NPs and air permeability. It can be seen from Table 10 that air permeability of the fabric is decreased after flame retardant MDPA coating, which is further decreased after ZnO NPs deposition. The untreated sample has an air permeability 701.40 mm/s, while sample B after MDPA treatment has an air permeability of 676.44 mm/s. The minimum air permeability was recorded for sample 23 which is 508.64 mm/s. Figure 16 shows that there is a gradual decrease in the air permeability with the increase in ZnO NPs deposition. The decrease in the permeability of air may have been a result of the reduction in the sizes of the pores in the fabric, which was caused by the development of ZnO NPs on the surface of the cotton fibers. However, there is no major collapse of air permeability. This range of air permeability is commercially acceptable.

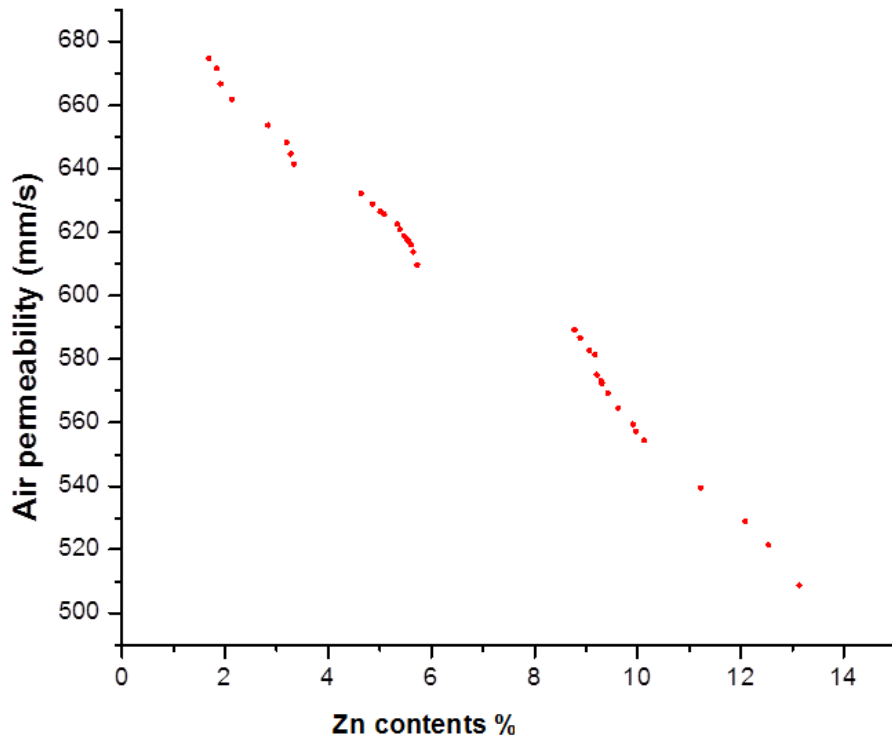


Figure 16. Graphical representation of air permeability against Zn contents %.

Table 10. Experimental results for air permeability.

Sample	Zinc acetate (M)	NaOH (M)	Sonication time (minutes)	MDPA (g/L)	Air permeability	
					mm/s	Std. dev.
Untreated	-	-	-	-	701.40	1.14
1	0.05	0.1	30	300	674.81	2.16
2	0.05	0.1	60	300	671.60	1.52
3	0.05	0.1	90	300	661.84	2.38
4	0.05	0.1	120	300	666.60	2.30
5	0.05	0.2	30	300	653.62	2.61
6	0.05	0.2	60	300	648.20	3.49
7	0.05	0.2	90	300	641.44	2.70
8	0.05	0.2	120	300	644.60	3.21
9	0.05	0.3	30	300	632.22	2.59
10	0.05	0.3	60	300	628.82	2.77
11	0.05	0.3	90	300	625.62	2.41
12	0.05	0.3	120	300	626.40	2.07
13	0.1	0.1	30	300	622.64	2.30
14	0.1	0.1	60	300	618.88	2.86
15	0.1	0.1	90	300	613.80	3.42
16	0.1	0.1	120	300	617.60	2.88
17	0.1	0.2	30	300	589.21	3.27
18	0.1	0.2	60	300	582.82	3.35
19	0.1	0.2	90	300	572.40	2.61
20	0.1	0.2	120	300	581.43	3.57
21	0.1	0.3	30	300	539.47	3.05
22	0.1	0.3	60	300	528.85	3.11
23	0.1	0.3	90	300	508.64	3.13
24	0.1	0.3	120	300	521.40	3.21
25	0.15	0.1	30	300	620.86	3.70
26	0.15	0.1	60	300	616.00	3.46
27	0.15	0.1	90	300	609.66	2.41
28	0.15	0.1	120	300	616.87	3.63
29	0.15	0.2	30	300	586.60	2.97
30	0.15	0.2	60	300	575.05	1.58
31	0.15	0.2	90	300	569.25	2.39
32	0.15	0.2	120	300	573.22	2.28
33	0.15	0.3	30	300	564.68	3.65
34	0.15	0.3	60	300	559.40	3.36
35	0.15	0.3	90	300	554.41	3.91
36	0.15	0.3	120	300	557.2	3.11
A	0.1	0.3	90 (magnetic stirring)	300	602.12	4.27
B	-	-	-	300	676.44	2.85

The regression model for predicting air permeability is depicted by equation (23). In order to assess the model's fit to the data, the R-squared value can be utilized. The model summary reveals that the R-

squared value indicates a capability of the fitted model to account for 73.76% of the total variations. Additionally, the model summary presents a p-value of 0.000 and an F-value of 81.06, implying the significance of the model.

$$\text{Air permeability (mm/s)} = 717.8 - 477 \text{ zinc acetate (M)} - 214.3 \text{ NaOH (M)} - 0.052 \text{ sonication time (minutes)} - 822 \text{ zinc acetate (M)} \times \text{NaOH (M)} - 0.03 \text{ zinc acetate (M)} \times \text{sonication time (minutes)} - 0.303 \text{ NaOH (M)} \times \text{sonication time (minutes)} \quad (23)$$

Model summary for air permeability

S = 22.713 R-squared = 73.76% R-squared (adj) = 72.86% R-squared (pred) = 71.82% F-value = 81.06 p-value = 0.000

5.14. Tensile strength

The measured values of tensile strength are shown in Table 11. It is apparent from Table 11 that after MDPA coating, both warp wise and weft wise tensile strength decreased. Furthermore, results presented in Table 11 show that after sonochemical treatment tensile strength further reduced in both warp wise and weft wise directions. Untreated fabric has warp wise and weft wise tensile strengths as 323.30 N and 247.83 N, respectively. While the sample B only coated with flame retardant chemical has warp wise tensile strength 284.78 N and weft wise tensile strength 216.12 N. The lowest tensile strength was recorded for sample 24 as 231.64 N and 182.06 N warp wise and weft wise respectively. Obtained results revealed that flame retardant coating, sonication time, and amount of Zn contents % all have a negative impact upon the tensile strength of the fabric. The decrease in tensile strength after the flame retardant application is due to the ester crosslinking of BTCA crosslinker present in the recipe with cellulose and acid degradation of cellulose due to BTCA[82]–[84]. Yang and Wei also reported that BTCA crosslinker reduces the strength of the cotton fabric due to acid-catalyzed depolymerization[85]. In another study Sadr and Montazer synthesized TiO₂ NPs on to the cotton fabric by sonochemical process and reported 3% loss in the fabric strength due to the effect of ultrasonic waves upon cellulose chains[35]. In one more research work Perincek *et al.* applied the ultrasonic method for cotton finishing and observed a little decrease in breaking strength of the fabric[86]. Parsad *et al.* investigated that ZnO NPs coating on to the cotton fabric increase the fabric friction and hence decrease the tensile strength[87]. Tania and Ali concluded that with increased amount of ZnO NPs deposition on to the cotton fabric resulted in decreased tensile strength[88]. The results are further in accordance with Attia *et al.* they reported a decrease in tensile strength of cotton/polyester blended fabric after ZnO NPs treatment[89].

Table 11. Experimental results for tensile strength.

Sample	Zinc acetate (M)	NaOH (M)	Sonication time (minutes)	MDPA (g/L)	Tensile strength (N)			
					Warp wise	Std. dev.	Weft wise	Std. dev.
Untreated	-	-	-	-	323.30	3.62	247.83	2.39
1	0.05	0.1	30	300	271.35	4.22	207.44	2.40
2	0.05	0.1	60	300	259.54	3.83	201.98	2.86
3	0.05	0.1	90	300	248.66	4.04	197.70	2.33
4	0.05	0.1	120	300	240.40	2.11	193.31	3.67
5	0.05	0.2	30	300	267.97	3.15	206.36	3.07
6	0.05	0.2	60	300	254.64	4.44	199.96	3.94
7	0.05	0.2	90	300	246.13	3.41	195.28	2.52
8	0.05	0.2	120	300	239.97	3.77	192.64	2.76
9	0.05	0.3	30	300	266.19	3.57	204.66	3.72
10	0.05	0.3	60	300	252.47	2.28	199.30	3.76
11	0.05	0.3	90	300	244.02	5.51	192.29	3.17
12	0.05	0.3	120	300	238.44	3.55	191.07	2.88
13	0.1	0.1	30	300	264.99	3.90	203.97	3.45
14	0.1	0.1	60	300	250.30	3.33	197.58	2.57
15	0.1	0.1	90	300	241.22	2.19	190.93	2.03
16	0.1	0.1	120	300	236.46	3.87	190.35	2.01
17	0.1	0.2	30	300	258.49	4.68	199.78	3.29
18	0.1	0.2	60	300	244.62	2.94	194.38	2.03
19	0.1	0.2	90	300	237.81	3.25	186.51	2.41
20	0.1	0.2	120	300	233.11	2.84	185.33	2.02
21	0.1	0.3	30	300	254.79	3.41	194.84	2.19
22	0.1	0.3	60	300	241.85	3.78	190.91	3.23
23	0.1	0.3	90	300	234.43	3.09	183.40	2.61
24	0.1	0.3	120	300	231.64	3.41	182.06	2.63
25	0.15	0.1	30	300	263.86	4.50	202.07	3.25
26	0.15	0.1	60	300	247.40	2.39	196.52	2.26
27	0.15	0.1	90	300	240.50	3.18	190.48	2.52
28	0.15	0.1	120	300	234.21	3.27	189.90	2.05
29	0.15	0.2	30	300	255.16	3.57	198.35	2.42
30	0.15	0.2	60	300	242.40	4.41	193.94	3.05
31	0.15	0.2	90	300	235.99	4.78	185.70	2.39
32	0.15	0.2	120	300	232.64	3.16	184.88	2.19
33	0.15	0.3	30	300	256.32	3.22	196.78	2.66
34	0.15	0.3	60	300	244.34	3.32	193.57	2.78
35	0.15	0.3	90	300	239.53	2.87	185.53	2.14
36	0.15	0.3	120	300	235.45	3.47	184.68	1.96
A	0.1	0.3	90 (magnetic stirring)	300	278.58	3.49	213.34	3.24
B	-	-	-	300	284.78	4.18	216.12	3.68

Equations (24) and (25) show the regression model used to determine tensile strength warp wise and weft wise respectively. According to the model summary, for warp wise tensile strength the fitted model can explain 82.42% of the total variances based on its R-squared value. Furthermore, the model summary for warp wise tensile strength indicates the model's significance with a p-value of 0.00 and an F-value of 135.15. According to the model summary, for weft wise tensile strength the fitted model can explain 77.27% of the total variances based on its R-squared value. The model summary for weft wise tensile strength indicates the model's significance with a p-value of 0.00 and an F-value of 98.03.

$$\text{Tensile strength (N) (warp wise)} = 290.90 - 128.30 \text{ zinc acetate (M)} - 52.60 \text{ NaOH (M)} - 0.3939 \text{ sonication time (minutes)} + 71.00 \text{ zinc acetate (M)} \times \text{NaOH (M)} + 0.421 \text{ zinc acetate (M)} \times \text{sonication time (minutes)} + 0.295 \text{ NaOH (M)} \times \text{sonication time (minutes)} \quad (24)$$

Model summary for tensile strength warp wise

S = 4.997 R-squared = 82.42% R-squared (adj) = 81.81% R-squared (pred) = 80.99% F-value = 135.15 p-value = 0.000

$$\text{Tensile strength (N) (weft wise)} = 216.62 - 57.0 \text{ zinc acetate (M)} - 19.6 \text{ NaOH (M)} - 0.1610 \text{ sonication time (minutes)} - 66.5 \text{ zinc acetate (M)} \times \text{NaOH (M)} + 0.053 \text{ zinc acetate (M)} \times \text{sonication time (minutes)} + 0.0034 \text{ NaOH (M)} \times \text{sonication time (minutes)} \quad (25)$$

Model summary for tensile strength weft wise

S = 3.452 R-squared = 77.27% R-squared (adj) = 76.48% R-squared (pred) = 75.14% F-value = 98.03 p-value = 0.000

5.15. Wash durability

Tables 12, 13, and 14 show the wash durability results after 5, 10 and 20 wash cycles for samples A, B and 23. The results show that there is a gradual decrease in Zn contents %, P contents %, flame retardancy, and functional properties of the sample after each wash cycle. However, in the case of ultrasonically optimized sample 23, there is enough Zn and P contents % even after 20 wash cycles. Although char length increased to 52 mm and LOI decreased to 29.61 after 20 wash cycles for sample 23, however, these values are excellent for flame retardancy. Sample 23 retained enough amounts of Zn contents % after 20 wash cycles and showed 100 % bacterial reduction for both S.aureus and E.coli bacteria. Sample 23 showed an excellent UPF value of 123.16 and color intensity 244.73 even after 20 wash cycles.

Table 12. Results of contents analysis after washing.

Contents (%)				
After 5 wash cycles				
Sample	Zn contents (%)	Std. dev.	P contents (%)	Std. dev.
Sample A	5.76	0.13	3.30	0.05
Sample B	-	-	3.48	0.06
Sample 23	11.38	0.08	3.11	0.05
After 10 wash cycles				
Sample	Zn contents (%)	Std. dev.	P contents (%)	Std. dev.
Sample A	4.74	0.17	3.13	0.04
Sample B	-	-	3.32	0.06
Sample 23	10.61	0.06	2.99	0.04
After 20 wash cycles				
Sample	(%)	Std. dev.	(%)	Std. dev.
Sample A	3.97	0.10	3.04	0.07
Sample B	-	-	3.24	0.05
Sample 23	10.17	0.12	2.93	0.04

Table 13. Results of flammability test and LOI after washing

Flammability test and LOI								
After 5 wash cycles								
Sample	After flame time (s)	Std. dev.	After glow time (s)	Std. dev.	Char length (mm)	Std. dev.	LOI	Std. dev.
Sample A	5.94	0.91	3.15	0.68	89	4.02	26.70	0.21
Sample B	10.32	0.37	5.47	0.28	134	5.24	22.11	0.18
Sample 23	0	0	0	0	46	0.94	30.32	0.13
After 10 wash cycles								
Sample	After flame time (s)	Std. dev.	After glow time (s)	Std. dev.	Char length (mm)	Std. dev.	LOI	Std. dev.
Sample A	7.03	1.01	3.52	0.74	93	4.36	24.91	0.32
Sample B	10.72	0.41	5.89	0.32	145	5.57	21.60	0.24
Sample 23	0	0	0	0	49	1.03	29.83	0.17
After 20 wash cycles								
Sample	After flame time (s)	Std. dev.	After glow time (s)	Std. dev.	Char length (mm)	Std. dev.	LOI	Std. dev.
Sample A	7.82	1.12	4.23	0.88	96	5.24	23.52	0.27
Sample B	11.29	0.69	6.08	0.51	149	5.93	20.41	0.23
Sample 23	0	0	0	0	52	1.36	29.61	0.11

Table 14. Results of antibacterial activity, UV protection, and self-cleaning after washing.

Bacterial reduction (%) , UPF and color intensity								
After 5 wash cycles								
Sample	S. aureus reduction %	Std. dev.	E.coli reduction %	Std. dev.	UPF	Std. dev.	Color intensity	Std. dev.
Sample A	72.43	6.38	70.28	4.81	41.37	5.29	209.53	6.42
Sample B	-	-	-	-	11.81	1.08	-	-
Sample 23	100	0	100	0	132.92	4.36	247.08	2.24
After 10 wash cycles								
Sample	S. aureus reduction %	Std. dev.	E.coli reduction %	Std. dev.	UPF	Std. dev.	Color intensity	Std. dev.
Sample A	63.23	3.69	60.96	4.16	34.87	3.35	190.24	5.12
Sample B	-	-	-	-	11.09	1.21	-	-
Sample 23	100	0	100	0	125.53	3.86	245.19	3.43
After 20 wash cycles								
Sample	S. aureus reduction %	Std. dev.	E.coli reduction %	Std. dev.	UPF	Std. dev.	Color intensity	Std. dev.
Sample A	54.47	4.65	50.52	3.73	30.76	2.57	187.39	4.71
Sample B	-	-	-	-	10.61	0.94	-	-
Sample 23	100	0	100	0	123.16	3.47	244.73	2.86

6. Evaluation of results and new findings

In this research study, cotton fabric was modified by the ultrasonically assisted in-situ synthesis of ZnO NPs and MDPA application by the conventional pad dry cure method. BTCA was used as a crosslinker for the crosslinking of MDPA with cellulose, so halogen and formaldehyde free ecological flame retardant treatment was done. The study revealed that MDPA greatly affects the flame retardant performance of the cotton fabric, which is further increases by the deposition of ZnO NPs. For the deposition of ZnO NPs onto the cotton fabric, sonication time and concentrations of the chemical

reagents were varied. The optimized conditions at 0.1 M zinc acetate, 0.3 M of NaOH, and 90 minutes of sonication time produced 13.14 % Zn contents. The pure hexagonal wurtzite crystalline structure of ZnO NPs was confirmed by XRD. The grafting and presence of ZnO NPs was confirmed by ICP AES, FTIR and SEM. While the presence of phosphorous contents was confirmed by ICP AES, and the grafting of phosphorous and amide group onto the cellulose structure was confirmed by FTIR. This research work disclosed that the concentration of ZnO NPs deposited onto the fabric has a direct correlation with flame retardancy and other functional properties. The optimized sample 23 showed excellent performance for flame retardancy before and after washing. A 100 % bacterial reduction for both *S. aureus* and *E. coli* bacteria was observed even after 20 wash cycles. The sample with the highest concentration of ZnO NPs showed UPF value of 143.76 initially and 123.16 after 20 wash cycles. Developed samples showed good photocatalytic self-cleaning before and after washing. The results obtained in this research work proved that ultrasonically developed fabric samples showed better flame retardancy and functional properties as compared to fabric sample developed by conventional magnetic stirring method. SEM analysis showed that the ultrasonic method deposits ZnO NPs onto the cotton fabric more uniformly and homogeneously as compared to the conventional magnetic stirring method. This research study revealed that MDPA application increased the bending rigidity of the fabric which was further increased by the deposition of ZnO NPs. On the other hand MDPA application resulted in a decrease in air permeability which further decrease after ZnO NPs deposition. In the case of tensile strength the developed samples showed less tensile strength as compared to the untreated sample, which was due to the ester crosslinking of BTCA crosslinker, the effect of ultrasonic waves upon cellulose chains, and the increase in the friction between the fabric structure due to the presence of ZnO NPs. However results showed that the air permeability and tensile strength of the developed samples are in an acceptable range.

Flame retardant multifunctional textiles at hand these days are the outcome of only chemical treatments; at present, the technology that has been developed for producing flame retardant textiles based on nanomaterial is still at the lab scale. The uses of nanoparticles impart some other desired properties. In future research should be center of attention on the application of nanoparticles as stuffing material, as their nano sizes let them penetrate into the interiors of polymer chains, hence imparting multifunctional properties. Along with ZnO NPs in the future other metal oxides NPs (e.g. TiO₂, CuO, MgO etc.) and the nano clay should also be used in combination with MDPA to obtain the best FR/NPs system.

7. References

- [1] S. Hall and B. Everts, "Fire Loss in the United States During 2021 (NFPA ®) Key Findings," no. September, 2022.
- [2] J. H. Troitzsch, "Fires, statistics, ignition sources, and passive fire protection measures," *J. Fire Sci.*, vol. 34, no. 3, pp. 171–198, 2016, doi: 10.1177/0734904116636642.
- [3] A. N. Zhang *et al.*, "Construction of durable eco-friendly biomass-based flame-retardant coating for cotton fabrics," *Chem. Eng. J.*, vol. 410, no. January, p. 128361, 2021, doi:

10.1016/j.cej.2020.128361.

- [4] V. Babrauskas, D. Lucas, D. Eisenberg, V. Singla, M. Dedeo, and A. Blum, “Flame retardants in building insulation: a case for re-evaluating building codes,” *Build. Res. Inf.*, vol. 40, no. 6, pp. 738–755, 2012.
- [5] S. A. H. Ravandi and M. Valizadeh, “Properties of fibers and fabrics that contribute to human comfort,” in *Improving comfort in clothing*, Elsevier, 2011, pp. 61–78.
- [6] J. Yip and W.-Y. Chan, “Textile fibers and fabrics,” in *Latest Material and Technological Developments for Activewear*, Elsevier, 2020, pp. 47–72.
- [7] H. A. Cheema, A. El-Shafei, and P. J. Hauser, “Conferring flame retardancy on cotton using novel halogen-free flame retardant bifunctional monomers: Synthesis, characterizations and applications,” *Carbohydr. Polym.*, vol. 92, no. 1, pp. 885–893, 2013, doi: 10.1016/j.carbpol.2012.09.081.
- [8] T. Mayer-Gall *et al.*, “A green water-soluble cyclophosphazene as a flame retardant finish for textiles,” *Molecules*, vol. 24, no. 17, pp. 26–28, 2019, doi: 10.3390/molecules24173100.
- [9] M. L. Rahman Liman, M. T. Islam, M. R. Repon, M. M. Hossain, and P. Sarker, “Comparative dyeing behavior and UV protective characteristics of cotton fabric treated with polyphenols enriched banana and watermelon biowaste,” *Sustain. Chem. Pharm.*, vol. 21, no. March, p. 100417, 2021, doi: 10.1016/j.scp.2021.100417.
- [10] Z. Fan, L. Di, X. Zhang, and H. Wang, “A surface dielectric barrier discharge plasma for preparing cotton-fabric-supported silver nanoparticles,” *Nanomaterials*, vol. 9, no. 7, 2019, doi: 10.3390/nano9070961.
- [11] K. K. Zhang *et al.*, “Improve the flame retardancy of cellulose fibers by grafting zinc ion,” *Carbohydr. Polym.*, vol. 136, pp. 121–127, 2016, doi: 10.1016/j.carbpol.2015.09.026.
- [12] S. Saleemi *et al.*, “Surface functionalization of cotton and pc fabrics using SiO₂ and ZnO nanoparticles for durable flame retardant properties,” *Coatings*, vol. 10, no. 2, 2020, doi: 10.3390/coatings10020124.
- [13] S. Yang, Y. Hu, and Q. Zhang, “Synthesis of a phosphorus–nitrogen-containing flame retardant and its application in epoxy resin,” *High Perform. Polym.*, vol. 31, no. 2, pp. 186–196, 2019, doi: 10.1177/0954008318756496.

- [14] T. N. Rao, T. M. Naidu, M. S. Kim, B. Parvatamma, Y. Prashanthi, and B. H. Koo, "Influence of zinc oxide nanoparticles and char forming agent polymer on flame retardancy of intumescent flame retardant coatings," *Nanomaterials*, vol. 10, no. 1, 2020, doi: 10.3390/nano10010042.
- [15] T. M. Nguyen, S. Chang, B. Condon, R. Slopek, E. Graves, and M. Yoshioka-Tarver, "Structural effect of phosphoramidate derivatives on the thermal and flame retardant behaviors of treated cotton cellulose," *Ind. Eng. Chem. Res.*, vol. 52, no. 13, pp. 4715–4724, 2013, doi: 10.1021/ie400180f.
- [16] J. Li, W. Jiang, and M. Liu, "Durable phosphorus/nitrogen flame retardant for cotton fabric," *Cellulose*, vol. 29, no. 8, pp. 4725–4751, 2022, doi: 10.1007/s10570-022-04558-x.
- [17] Y. Chen, L. Xu, X. Wu, and B. Xu, "The influence of nano ZnO coated by phosphazene/triazine bi-group molecular on the flame retardant property and mechanical property of intumescent flame retardant poly (lactic acid) composites," *Thermochim. Acta*, vol. 679, no. 11, 2019, doi: 10.1016/j.tca.2019.178336.
- [18] N. T. Huong, V. T. H. Khanh, and N. P. D. Linh, "Optimizing content of Pyrovatex CP New and Knittex FFRC in flame retardant treatment for cotton fabric," *Ind. Textila*, vol. 72, no. 3, pp. 315–323, 2021, doi: 10.35530/IT.072.03.1648.
- [19] S. C. Chang, B. Condon, J. Smith, and S. Nam, "Flame Resistant Cotton Fabric Containing Casein and Inorganic Materials Using an Environmentally-Friendly Microwave Assisted Technique," *Fibers Polym.*, vol. 21, no. 10, pp. 2246–2252, 2020, doi: 10.1007/s12221-020-9965-x.
- [20] I. Yaqoob, Asim ALI Parveen, Tabassum Umar, Khalid Nasir, Mohammad Nasir, "Role of Nanomaterials in the Treatment of waste water," *Water 2020*, vol. 12, p. 495, 2020.
- [21] A. A. Yaqoob *et al.*, "Recent Advances in Metal Decorated Nanomaterials and Their Various Biological Applications: A Review," *Front. Chem.*, vol. 8, no. May, pp. 1–23, 2020, doi: 10.3389/fchem.2020.00341.
- [22] A. R. Galaly and N. Dawood, "Non-Thermal Plasma Treatment Coupled with a Photocatalyst for Antimicrobial Performance of Ihram Cotton Fabric," *Nanomaterials*, vol. 12, no. 6, pp. 1–14, 2022, doi: 10.3390/nano12061004.

- [23] A. Javed *et al.*, “One step in-situ synthesis of zinc oxide nanoparticles for multifunctional cotton fabrics,” *Materials (Basel)*, vol. 14, no. 14, p. 3956, 2021.
- [24] A. V. Abramova *et al.*, “Strong antibacterial properties of cotton fabrics coated with ceria nanoparticles under high-power ultrasound,” *Nanomaterials*, vol. 11, no. 10, 2021, doi: 10.3390/nano11102704.
- [25] M. Fernandes *et al.*, “Polysaccharides and Metal Nanoparticles for Functional Textiles: A Review,” *Nanomaterials*, vol. 12, no. 6, p. 1006, 2022, doi: 10.3390/nano12061006.
- [26] D. Press, “Titanium dioxide and zinc oxide nanoparticles in sunscreens : focus on their safety and effectiveness,” pp. 95–112, 2011.
- [27] M. A. Tănase *et al.*, “Facile in situ synthesis of zno flower-like hierarchical nanostructures by the microwave irradiation method for multifunctional textile coatings,” *Nanomaterials*, vol. 11, no. 10, 2021, doi: 10.3390/nano11102574.
- [28] H. T. P. Nguyen *et al.*, “Characterization and photocatalytic activity of new photocatalysts based on Ag, F-modified ZnO nanoparticles prepared by thermal shock method,” *Arab. J. Chem.*, vol. 13, no. 1, pp. 1837–1847, 2020, doi: 10.1016/j.arabjc.2018.01.018.
- [29] P. J. P. Espitia, N. de F. F. Soares, J. S. dos R. Coimbra, N. J. de Andrade, R. S. Cruz, and E. A. A. Medeiros, “Zinc Oxide Nanoparticles: Synthesis, Antimicrobial Activity and Food Packaging Applications,” *Food Bioprocess Technol.*, vol. 5, no. 5, pp. 1447–1464, 2012, doi: 10.1007/s11947-012-0797-6.
- [30] A. Moezzi, A. M. McDonagh, and M. B. Cortie, “Zinc oxide particles: Synthesis, properties and applications,” *Chem. Eng. J.*, vol. 185–186, pp. 1–22, 2012, doi: 10.1016/j.cej.2012.01.076.
- [31] R. D. Kale, M. Soni, and T. Potdar, “A flame retardant, antimicrobial and UV protective polyester fabric by solvent crazing route,” *J. Polym. Res.*, vol. 26, no. 8, 2019, doi: 10.1007/s10965-019-1849-7.
- [32] M. M. A. El-Hady, A. Farouk, and S. Sharaf, “Flame retardancy and UV protection of cotton based fabrics using nano ZnO and polycarboxylic acids,” *Carbohydr. Polym.*, vol. 92, no. 1, pp. 400–406, 2013, doi: 10.1016/j.carbpol.2012.08.085.
- [33] E. Magovac, B. Vončina, I. Jordanov, J. C. Grunlan, and S. Bischof, “Layer-by-Layer

- Deposition: A Promising Environmentally Benign Flame-Retardant Treatment for Cotton, Polyester, Polyamide and Blended Textiles,” *Materials (Basel)*, vol. 15, no. 2, 2022, doi: 10.3390/ma15020432.
- [34] A. Javed, M. Azeem, J. Wiener, M. Thukkaram, J. Saskova, and T. Mansoor, “Ultrasonically Assisted In Situ Deposition of ZnO Nano Particles on Cotton Fabrics for Multifunctional Textiles,” *Fibers Polym.*, 2021, doi: 10.1007/s12221-021-0051-9.
- [35] F. Akhavan Sadr and M. Montazer, “In situ sonosynthesis of nano TiO₂ on cotton fabric,” *Ultrason. Sonochem.*, vol. 21, no. 2, pp. 681–691, 2014, doi: 10.1016/j.ultsonch.2013.09.018.
- [36] C. F. Putri and N. Tjahjono, “Counseling and application of personal protective equipment to reduce work accidents in welding workshops,” *Abdimas J. Pengabd. Masy. Univ. Merdeka Malang*, vol. 7, no. 3, pp. 460–470, 2022, doi: 10.26905/abdimas.v7i3.7016.
- [37] H. Nakashima, A. Utsunomiya, J. Takahashi, N. Fujii, and T. Okuno, “Hazard of ultraviolet radiation emitted in gas metal arc welding of mild steel,” *J. Occup. Health*, vol. 58, no. 5, pp. 452–459, 2016, doi: 10.1539/joh.16-0065-OA.
- [38] J. Ran, M. He, W. Li, D. Cheng, and X. Wang, “Growing ZnO nanoparticles on polydopamine-templated cotton fabrics for durable antimicrobial activity and UV protection,” *Polymers (Basel)*, vol. 10, no. 5, 2018, doi: 10.3390/polym10050495.
- [39] J. Wojnarowicz, T. Chudoba, and W. Lojkowski, “A Review of Microwave Synthesis of Zinc Oxide Nanomaterials : Reactants , Process Parameters and Morphologies,” 2020.
- [40] A. Mohajerani *et al.*, “Nanoparticles in construction materials and other applications, and implications of nanoparticle use,” *Materials (Basel)*, vol. 12, no. 19, p. 3052, 2019.
- [41] A. C. Dodd, A. J. McKinley, M. Saunders, and T. Tsuzuki, “Effect of particle size on the photocatalytic activity of nanoparticulate zinc oxide,” *J. Nanoparticle Res.*, vol. 8, no. 1, pp. 43–51, 2006, doi: 10.1007/s11051-005-5131-z.
- [42] L. Jiao, J. Ma, and H. Dai, “Preparation and characterization of self-reinforced antibacterial and oil-resistant paper using a NaOH/Urea/ZnO solution,” *PLoS One*, vol. 10, no. 10, pp. 1–16, 2015, doi: 10.1371/journal.pone.0140603.
- [43] X. Z. Sun, D. H. Bremner, N. Wan, and X. Wang, “Development of antibacterial ZnO-loaded cotton fabric based on in situ fabrication,” *Appl. Phys. A Mater. Sci. Process.*, vol. 122, no. 11,

- pp. 1–9, 2016, doi: 10.1007/s00339-016-0482-0.
- [44] V. H. T. Thi and B.-K. Lee, “Development of multifunctional self-cleaning and UV blocking cotton fabric with modification of photoactive ZnO coating via microwave method,” *J. Photochem. Photobiol. A Chem.*, vol. 338, pp. 13–22, 2017.
- [45] D. Shao, Y. Gao, K. Cao, and Q. Wei, “Rapid surface functionalization of cotton fabrics by modified hydrothermal synthesis of ZnO,” *J. Text. Inst.*, vol. 108, no. 8, pp. 1391–1397, 2017.
- [46] P. M. Sivakumar, S. Balaji, V. Prabhawathi, R. Neelakandan, P. T. Manoharan, and M. Doble, “Effective antibacterial adhesive coating on cotton fabric using ZnO nanorods and chalcone,” *Carbohydr. Polym.*, vol. 79, no. 3, pp. 717–723, 2010, doi: 10.1016/j.carbpol.2009.09.027.
- [47] C. Chung, M. Lee, and E. K. Choe, “Characterization of cotton fabric scouring by FT-IR ATR spectroscopy,” *Carbohydr. Polym.*, vol. 58, no. 4, pp. 417–420, 2004, doi: 10.1016/j.carbpol.2004.08.005.
- [48] H. Zhao, Q. Liang, and Y. Lu, “Microstructure and properties of copper plating on citric acid modified cotton fabric,” *Fibers Polym.*, vol. 16, no. 3, pp. 593–598, 2015, doi: 10.1007/s12221-015-0593-9.
- [49] F. Xu, G. Zhang, P. Wang, and F. Dai, “Durable and high-efficiency casein-derived phosphorus-nitrogen-rich flame retardants for cotton fabrics,” *Cellulose*, vol. 29, no. 4, pp. 2681–2697, 2022, doi: 10.1007/s10570-022-04430-y.
- [50] P. Bazant, I. Kuritka, L. Munster, and L. Kalina, “Microwave solvothermal decoration of the cellulose surface by nanostructured hybrid Ag/ZnO particles: a joint XPS, XRD and SEM study,” *Cellulose*, vol. 22, no. 2, pp. 1275–1293, 2015, doi: 10.1007/s10570-015-0561-y.
- [51] Ö. Ceylan, L. Van Landuyt, H. Rahier, and K. De Clerck, “The effect of water immersion on the thermal degradation of cotton fibers,” *Cellulose*, vol. 20, no. 4, pp. 1603–1612, 2013, doi: 10.1007/s10570-013-9936-0.
- [52] H. Barani, “Surface activation of cotton fiber by seeding silver nanoparticles and in situ synthesizing ZnO nanoparticles,” *New J. Chem.*, vol. 38, no. 9, pp. 4365–4370, 2014, doi: 10.1039/c4nj00547c.
- [53] S. Gaan and G. Sun, “Effect of phosphorus and nitrogen on flame retardant cellulose: a study of phosphorus compounds,” *J. Anal. Appl. Pyrolysis*, vol. 78, no. 2, pp. 371–377, 2007.

- [54] M. H. Fallah, S. A. Fallah, and M. A. Zanjanchi, "Synthesis and characterization of nano-sized zinc oxide coating on cellulosic fibers: Photoactivity and flame-retardancy study," *Chinese J. Chem.*, vol. 29, no. 6, pp. 1239–1245, 2011, doi: 10.1002/cjoc.201190230.
- [55] W. Wu, X. Zhen, and C. Q. Yang, "Correlation between Limiting Oxygen Index and Phosphorus Content of the Cotton Fabric Treated with a Hydroxy-functional Organophosphorus Flame Retarding Finish and Melamine-Formaldehyde," *J. Fire Sci.*, vol. 22, no. 1, pp. 11–23, 2004, doi: 10.1177/0734904104035253.
- [56] S. Wang *et al.*, "Durable flame retardant finishing of cotton fabrics with organosilicon functionalized cyclotriphosphazene," *Polym. Degrad. Stab.*, vol. 128, pp. 22–28, 2016, doi: 10.1016/j.polymdegradstab.2016.02.009.
- [57] X. Qian *et al.*, "Combustion and thermal degradation mechanism of a novel intumescent flame retardant for epoxy acrylate containing phosphorus and nitrogen," *Ind. Eng. Chem. Res.*, vol. 50, no. 4, pp. 1881–1892, 2011.
- [58] P. Dhandapani, A. S. Siddarth, S. Kamalasekaran, S. Maruthamuthu, and G. Rajagopal, "Bio-approach: Ureolytic bacteria mediated synthesis of ZnO nanocrystals on cotton fabric and evaluation of their antibacterial properties," *Carbohydr. Polym.*, vol. 103, no. 1, pp. 448–455, 2014, doi: 10.1016/j.carbpol.2013.12.074.
- [59] A. Siriviriyanun, E. A. O'Rear, and N. Yanumet, "Self-extinguishing cotton fabric with minimal phosphorus deposition," *Cellulose*, vol. 15, no. 5, pp. 731–737, 2008, doi: 10.1007/s10570-008-9223-7.
- [60] S. Gaan, G. Sun, K. Hutches, and M. H. Engelhard, "Effect of nitrogen additives on flame retardant action of tributyl phosphate: phosphorus–nitrogen synergism," *Polym. Degrad. Stab.*, vol. 93, no. 1, pp. 99–108, 2008.
- [61] A. R. Horrocks, B. K. Kandola, P. J. Davies, S. Zhang, and S. A. Padbury, "Developments in flame retardant textiles—a review," *Polym. Degrad. Stab.*, vol. 88, no. 1, pp. 3–12, 2005.
- [62] E. D. Tomak and A. D. Cavdar, "Limited oxygen index levels of impregnated Scots pine wood," *Thermochim. Acta*, vol. 573, pp. 181–185, 2013, doi: 10.1016/j.tca.2013.09.022.
- [63] J. Alongi, *Update on flame retardant textiles*. Smithers Rapra, 2013.
- [64] Y.-W. Wang, R. Shen, Q. Wang, and Y. Vasquez, "ZnO microstructures as flame-retardant

- coatings on cotton fabrics,” *ACS omega*, vol. 3, no. 6, pp. 6330–6338, 2018.
- [65] A. Arputharaj, V. Nandanatham, and S. R. Shukla, “A simple and efficient protocol to develop durable multifunctional property to cellulosic materials using in situ generated nano-ZnO,” *Cellulose*, vol. 24, pp. 3399–3410, 2017.
- [66] A. K. Samanta, R. Bhattacharyya, S. Jose, G. Basu, and R. Chowdhury, “Fire retardant finish of jute fabric with nano zinc oxide,” *Cellulose*, vol. 24, no. 2, pp. 1143–1157, 2017, doi: 10.1007/s10570-016-1171-z.
- [67] K. Xie, A. Gao, and Y. Zhang, “Flame retardant finishing of cotton fabric based on synergistic compounds containing boron and nitrogen,” *Carbohydr. Polym.*, vol. 98, no. 1, pp. 706–710, 2013.
- [68] L. Wang, C. Hu, and L. Shao, “The antimicrobial activity of nanoparticles: Present situation and prospects for the future,” *Int. J. Nanomedicine*, vol. 12, pp. 1227–1249, 2017, doi: 10.2147/IJN.S121956.
- [69] S. Shaikh *et al.*, “Mechanistic insights into the antimicrobial actions of metallic nanoparticles and their implications for multidrug resistance,” *Int. J. Mol. Sci.*, vol. 20, no. 10, pp. 1–15, 2019, doi: 10.3390/ijms20102468.
- [70] K. Han and M. Yu, “Study of the preparation and properties of UV-blocking fabrics of a PET/TiO₂ nanocomposite prepared by in situ polycondensation,” *J. Appl. Polym. Sci.*, vol. 100, no. 2, pp. 1588–1593, 2006.
- [71] S. Mondal, “Nanomaterials for UV protective textiles,” *J. Ind. Text.*, vol. 0, no. 0, pp. 1–30, 2021, doi: 10.1177/1528083721988949.
- [72] O. K. Alebeid and T. Zhao, “Review on: developing UV protection for cotton fabric,” *J. Text. Inst.*, vol. 108, no. 12, pp. 2027–2039, 2017, doi: 10.1080/00405000.2017.1311201.
- [73] A. Verbič, M. Gorjanc, and B. Simončič, “Zinc oxide for functional textile coatings: Recent advances,” *Coatings*, vol. 9, no. 9, pp. 17–23, 2019, doi: 10.3390/coatings9090550.
- [74] A. Bashari, M. Shakeri, and A. R. Shirvan, “UV-protective textiles,” in *The impact and prospects of green chemistry for textile technology*, Elsevier, 2019, pp. 327–365.
- [75] H. Sudrajat, “Superior photocatalytic activity of polyester fabrics coated with zinc oxide from

- waste hot dipping zinc,” *J. Clean. Prod.*, vol. 172, pp. 1722–1729, 2018, doi: 10.1016/j.jclepro.2017.12.024.
- [76] J. Bedia, V. Muelas-Ramos, M. Peñas-Garzón, A. Gómez-Avilés, J. J. Rodríguez, and C. Belver, “A review on the synthesis and characterization of metal organic frameworks for photocatalytic water purification,” *Catalysts*, vol. 9, no. 1, p. 52, 2019.
- [77] M. Shaban, S. Abdallah, and A. A. Khalek, “Characterization and photocatalytic properties of cotton fibers modified with ZnO nanoparticles using sol–gel spin coating technique,” *Beni-Suef Univ. J. Basic Appl. Sci.*, vol. 5, no. 3, pp. 277–283, 2016, doi: 10.1016/j.bjbas.2016.08.003.
- [78] L. Fridrichová, “A new method of measuring the bending rigidity of fabrics and its application to the determination of the their anisotropy,” *Text. Res. J.*, vol. 83, no. 9, pp. 883–892, 2013, doi: 10.1177/0040517512467133.
- [79] M. Z. Khan *et al.*, “Ultra-fast growth of ZnO nanorods on cotton fabrics and their self-cleaning and physiological comfort properties,” *Coatings*, vol. 11, no. 11, p. 1309, 2021.
- [80] I. S. Tania and M. Ali, “Coating of ZnO nanoparticle on cotton fabric to create a functional textile with enhanced mechanical properties,” *Polymers (Basel)*, vol. 13, no. 16, p. 2701, 2021.
- [81] L. Hes and M. de Araujo, “Simulation of the effect of air gaps between the skin and a wet fabric on resulting cooling flow,” *Text. Res. J.*, vol. 80, no. 14, pp. 1488–1497, 2010.
- [82] W. Sricharussin, W. Ryo-Aree, W. Intasen, and S. Pongraksakirt, “Effect of boric acid and BTCA on tensile strength loss of finished cotton fabrics,” *Text. Res. J.*, vol. 74, no. 6, pp. 475–480, 2004.
- [83] J. Wal. Wang, J.; Fang, K.; Liu, X.; Zhang, S.; Qiao, X.; Liu, D. A Review on the Status of Formaldehyde-Free Anti-Wrinkle Cross-Linking Agents for Cotton Fabrics: Mechanisms and Applications. *Ind. Crops Prod.* 2023, 200, 116831, doi:101.
- [84] B. Ji, C. Zhao, K. Yan, and G. Sun, “Effects of acid diffusibility and affinity to cellulose on strength loss of polycarboxylic acid crosslinked fabrics,” *Carbohydr. Polym.*, vol. 144, pp. 282–288, 2016.
- [85] C. Q. Yang, W. Wei, and G. C. Lickfield, “Mechanical strength of durable press finished cotton fabric: Part II: Comparison of crosslinking agents with different molecular structures and reactivity,” *Text. Res. J.*, vol. 70, no. 2, pp. 143–147, 2000.

- [86] S. Perincek, I. Bahtiyari, A. Korlu, and K. Duran, “New techniques in cotton finishing,” *Text. Res. J.*, vol. 79, no. 2, pp. 121–128, 2009.
- [87] A. Yadav *et al.*, “Functional finishing in cotton fabrics using zinc oxide nanoparticles,” *Bull. Mater. Sci.*, vol. 29, pp. 641–645, 2006.
- [88] I. S. Tania and M. Ali, “Effect of the coating of zinc oxide (ZnO) nanoparticles with binder on the functional and mechanical properties of cotton fabric,” *Mater. Today Proc.*, vol. 38, pp. 2607–2611, 2020, doi: 10.1016/j.matpr.2020.08.171.
- [89] N. F. Attia, M. Moussa, A. M. F. Sheta, R. Taha, and H. Gamal, “Effect of different nanoparticles based coating on the performance of textile properties,” *Prog. Org. Coatings*, vol. 104, pp. 72–80, 2017, doi: 10.1016/j.porgcoat.2016.12.007.

8. List of Publications

Journal publications

- Javed, A., Wiener, J., Saskova, J., & Müllerová, J. (2022). Zinc Oxide Nanoparticles (ZnO NPs) and N-Methylol Dimethyl Phosphonopropion Amide (MDPA) System for Flame Retardant Cotton Fabrics. *Polymers*, 14(16), 3414. (Impact Factor 5.0)
- Javed, A., Wiener, J., Tamulevičienė, A., Tamulevičius, T., Lazauskas, A., Saskova, J., & Račkauskas, S. (2021). One step in-situ synthesis of zinc oxide nanoparticles for multifunctional cotton fabrics. *Materials*, 14(14), 3956. (Impact Factor 3.748)
- Javed, A., Azeem, M., Wiener, J., Thukkaram, M., Saskova, J., & Mansoor, T. (2021). Ultrasonically Assisted In Situ Deposition of ZnO Nano Particles on Cotton Fabrics for Multifunctional Textiles. *Fibers and Polymers*, 22(1), 77-86. (Impact Factor 2.5)
- Khan, M. Z., Militky, J., Petru, M., Tomková, B., Ali, A., Javed, A., & Křemenáková, D. (2021). Ultra-Fast Growth of ZnO Nanorods on Cotton Fabrics and Their Self-Cleaning and Physiological Comfort Properties. *Coatings*, 11(11), 1309. (Impact Factor 3.4)
- Azeem, M., Javed, A., Morikawa, H., Noman, M. T., Khan, M. Q., Shahid, M., & Wiener, J. (2021). Hydrophilization of polyester textiles by nonthermal plasma. *Autex Research Journal*, 21(2), 142-149. (Impact Factor 1.944)
- Mansoor, T., Hes, L., Skenderi, Z., Siddique, H. F., Hussain, S., & Javed, A. (2019). Effect of preheat setting process on heat, mass and air transfer in plain socks. *The journal of the Textile Institute*, 110(2), 159-170. (Impact Factor 2.17).

- Fraz, A., Azeem, M., & Javed, A. (2018). Effect of Dyeing Temperature on the Shrinkage and Fastness Properties of Polyester/Acrylic Fabric. *Pakistan Journal of Scientific & Industrial Research Series A: Physical Sciences*, 61(2), 100-105. (Impact Factor 0.679)

Conference publications

- Javed, A., Wiener, J., Saskova. (2024). N-Methylol Dimethyl Phosphonopropion Amide (MDPA) and Zinc Oxide Nanoparticles (ZnO NPs) coated Flame Retardant Cotton Fabric. In *Proceedings of the autex 2024 world conference*. 17-19 June, 2024, Liberec, Czech Republic.
- Javed, A., Wiener, J., & Saskova, J. (2023). Sonochemical Route to Develop Flame Retardant Cotton Fabrics with Multifunctional Properties. In *Proceedings of The Fiber Society 2023 Fall Meeting and Technical Conference Sustainability, Scalability, and Society: Advanced Fibers and Textiles*. October 25–27, 2023, Drexel University, Philadelphia, Pennsylvania, USA.
- Javed, A., Wiener, J., Saskova, J., & Militky, J. (2022). In-situ green synthesis of zinc oxide nanoparticles (ZnO NPs) onto the cotton fabrics by neem (*azadirachta indica*) leaf extract. In *Proceedings of the 21th World Textile Conference-Autex 2022*. Lodz, Poland.
- Javed, A., Wiener, J., Saskova, J., & Militky, J. (2021). In-situ sonochemical synthesis of ZnO on cotton fabrics for antibacterial and self-cleaning properties. In *Proceedings of the 20th World Textile Conference-Autex 2021*. Guimarães, Portugal.
- Javed, A., Musaddaq, A., & Šašková, J. (2019). UV protective fabrics by application of ball milled Neem tree leaves. In *Proceedings the 19th World Textile Conference-Autex 2019*. Ghent, Belgium.
- Azeem, M., Javed, A., & Wiener, J. (2019). Hydrophilization of PET using DBD plasma. In *proceedings: ICCM22 2019*. Melbourne, VIC: Engineers Australia, 2019: 430-436.
- Mansoor, T., Hes, L., Skenderi, Z. S., & Javed, A. (2018). Effect of moisture content on thermophysiological properties of plain knitted socks followed by thermal resistance comparison among different skin models. In *proceedings 22nd STRUTEX conference 2018*, Liberec, Czech Republic.

Curriculum Vitae

Personal Information



Asif Javed M.Sc.

Erbenova 123/18 Liberec 8 46008

Liberec, Czech Republic.

+420775465828

mianasif58@gmail.com

Date of birth: 27th July 1981

Nationality: Pakistani

Education

Doctoral student (April 2017-until now)

Department of Material Engineering, Faculty of Textile Engineering
Technical University of Liberec, Czech Republic.

M.Sc. fibre technology (September 2005 to July 2009)

Department of Fibre & Textile Technology, Faculty of Agricultural
Engineering & Technology, University of Agriculture Faisalabad,
Pakistan.

Work experience

Assistant Manager Dyeing Process Team (May 2010 to March 2017)

Masood Textile Mills Ltd. Faisalabad Pakistan

Internship

- Department of Textile and Clothing Engineering, University of Ljubljana, Slovenia. (25 May 2018 to 25 July 2018).
- Department of Materials, Textiles and Chemical Engineering (Match), Gent University, Belgium. (27 June 2019 to 26 September 2019).
- Institute of Materials Science, Kaunas University of Technology, Lithuania. (10 February 2020 to 11 June 2020).

Recommendation of Supervisor

FAKULTA TEXTILNÍ TUL



Supervisor's thesis's evaluation for the PhD thesis of Mr.Asif Javed M.Sc.

Title of thesis

Development of Flame Retardant Cotton Fabrics with Multifunctional Properties

Presented dissertation thesis is aimed on development of flame retardant cotton fabrics with can provide multifunctional properties. Main topic was to develop a halogen and formaldehyde free ecological flame retardant fabric along with multifunctional properties. The zinc oxide nanoparticles were used in this work and applied by the sonochemical method. Treated (developed) samples showed very good results for flame retardancy, LOI, UPF, antibacterial activity and self- cleaning.

The thesis is well written, concise and compact. Candidate has done all work systematically on required scientific level, results are presented logical and understable, conclusions of thesis are interesting and novel.

Publication activities of student are in very good level - 3 papers (first author) has been published in impacted journals during his research work, as like as a range of publications at international conferences including conferences like AUTEX or Fiber Society conference were presented. Student also participated in other research works, which is evident by other six publications of which he is a co-author.

I recommend the thesis for final defense

Liberec 7/10/2024

Ing. Jana Šašková Ph.D

(Supervisor)

Reviews of the Opponents

Referee's report
on PhD. thesis of
Asif Javed

“Development of Flame Retardant Cotton Fabrics with Multifunctional Properties”

by
Doc. Ing. Stanislav Petrik, CSc.

The thesis consists of 141 pages divided into 6 chapters. The aim of the thesis was to develop a halogen and formaldehyde free ecological and durable flame retardant fabric possessing multifunctional properties and to find optimal conditions and parameters for its preparation. ZnO nanoparticles have been studied as the main functional surface additive. Besides the flame retardant parameters of the samples, properties as UV protection, antibacterial activity, self-cleaning, comfort-related parameters (bending rigidity, air permeability) and durability (tensile strength, wash resistance) have been measured and discussed.

The thesis has standard parts - Introduction, Aim and Objectives, Literature Review, Materials and Methods, Results and Discussion, Summary and Future Prospective. At the end, there are References and a List of author's publications. The author's record of publications is very good.

First pages

Before the introduction, there are Contents, List of tables, List of figures, List of abbreviations. These lists contain almost all type of contents complete.

Thesis significance, scope and objectives

The author made an introduction to his work and explained the objectives of the study. The topic of the work is very actual and necessary, as the flame retardant textiles used currently are mostly based on polymers and the flame retardants are environmentally unfriendly. Several side effects and properties of the chosen solution (i.e. antibacterial and self-cleaning effects) promise additional benefits and make a sense. However, in the Chapter 2, I am missing wider context of the aim and objectives, which are focused on concrete research steps only.

Literature review

There is a sufficient number of literature sources divided into 13 parts. The whole chapter is well written. The labelling of all figures is clear. The literature part well explained previous work and the most critical literature findings are related to the topic, leading to logical consequences with the author's work.

Methodology

The methods author used are essential for the final topic of the thesis. Materials and methods are appropriately described, with sufficient degree of understanding demonstrated. The choice of the materials and methods corresponds to the objectives of the work and showed later good relevance to obtained results.

Results and discussion

The chapter summarizes all results of the thesis. For each series of samples, several measurements were performed – Zn and P content, vertical flame retardant test, SEM, particle size, XRD, FTIR and thermo-gravimetric analysis, antibacterial activity, durability of fabrics, etc. The results are presented in both table and graph forms, with visible trends, which are critically analysed and logically interpreted. Error bars might be effective especially for Fig. 33 through 35.

Summary and future prospective

This chapter summarizes the findings of the previous chapters. The author presents interesting results of experimental work in the field of development of flame retardant bio-base fabrics. The doctoral student demonstrated good scientific work and published his results sufficiently. The author summarizes most important achievements of the work as concrete values of the parameters of the textile samples. Also, he proposed future focus of the research in the field. However, more general structured conclusions in relation to the individual thesis objectives from Chapter 2 are missing.

Referee remarks, questions and conclusions

1. The thesis topic, focus, methodology and results are very consistent, following the objectives, well formulated and argued.
2. Hydrophilicity is one of the most important features of the cotton fabrics. Can you please provide any data how your flame retardant treatment affects this property?
3. Please comment on the partial comfort degradation (bending rigidity, air permeability?) of the cotton fabric caused by your flame retardant treatment. Did you make any tactile (or similar) tests verifying how users/people would “feel” the difference between standard and treated fabric?
4. Can you please compare the achieved flame retardant parameters of your samples with the ones of commercially available textiles (provide a basic benchmarking)?
5. Please discuss the possible application field of the materials you develop (clothing, automotive, aircraft, aerospace). Which flame retardant category/norm should your material fulfil?

Referee’s conclusion

The presented thesis of Asif Javed contains all the formal parts and shows the author is able to carry out scientific work. The author also showed good understanding of chemical processes applied in the thesis. The language is acceptable and entirely understandable.

The thesis meets the criteria, I recommend it to be taken to the defense.

In Liberec on August 29, 2024

doc. Ing. Stanislav Petřík, CSc.

Technical University in Liberec

Opponents review for the degree of Doctor of Philosophy defence

Candidate: Asif Javed, M.Sc.

Thesis title: Development of flame-retardant cotton fabrics with multifunctional properties

Thesis tutor: Ing. Jana Šašková, Ph.D.

Study subject: Textile Engineering

This opponent's review was written based on request of doc. Ing. Vladimír Bajžík, Ph.D. – dean of the Faculty of Textile, ref. no. TUL-24/4114/039208 of June 25, 2024.

General information: Thesis is composed from 6 chapters, total of 140 A4 pages. Thesis structure is based on commented individual chapters dealing with the introduction, definition of the objectives, state of the art of the matter under study, experimental, results and discussion, summary and conclusions. Totally there was cited 271 references. Thesis were written in English language.

- 1. The nature and scope of the investigation:** The thesis addresses an important scientific and technical problem related to the application, processing, and manufacturing of ecological, halogen, and formaldehyde-free flame-retardant cotton-based fabrics. The study is rooted in applied materials engineering. Zinc oxide nanoparticles were attached to the cotton fabric surface using a sonochemical method, with zinc acetate dihydrate and sodium hydroxide serving as precursors. The flame-retardant N-methylol dimethylphosphonopropionamide (MDPA) was applied to this surface and crosslinked using 1,2,3,4-butanetetracarboxylic acid (BTCA), with sodium hypophosphite (SHP) acting as the catalyst. Comprehensive material engineering and physicochemical analyses of the prepared fabrics were conducted, including ICP-AES, XRD, SEM, and FTIR. Additionally, a series of vertical flame-retardant tests were performed.
- 2. The contribution made to the subject field, including the extent to which the thesis contains original, publishable work of merit:** The results obtained are an original contribution to the study of novel composite structure preparation, manufacturing, and material characterization. The author has rigorously analysed and compared a wide range of physicochemical and material characteristics and their interdependencies. The thesis represents a complex experimental study with excellent theoretical data evaluation and analysis. The results from this study provide new, valuable insights into the field of applied materials science and engineering. The student has published most of the results in prestigious scientific journals specializing in materials engineering, materials science, and textile materials, including *Polymers*, *Materials*, *Fibers and Polymers*, *Coatings*, *Autex Research Journal*, and the *Pakistan Journal of Scientific and Industrial Research Series A: Physical Sciences*. The applicant has also presented findings at numerous scientific conferences, with six contributions. Most of the papers have successfully undergone rigorous peer review processes in these journals.

- 3. The quality of the submission and, where appropriate, of the investigative work described:** The presented Ph.D. thesis meets the usual quality standards in terms of content, presentation, data analysis, and interpretation. Therefore, I fully support the submission of this thesis as a basis for the final examination. The Ph.D. thesis meets the standard quality requirements for such a degree.

Question to be answered during the defence of the thesis: Did you characterize the durability of the developed fabric fire retardant coatings against frictional wear?

Signed: Doc. Mgr. Barbora Lapčíková, PhD.

Date: August 2, 2024